Cell

Genetic requirements for cell division in a genomically minimal cell

Graphical abstract

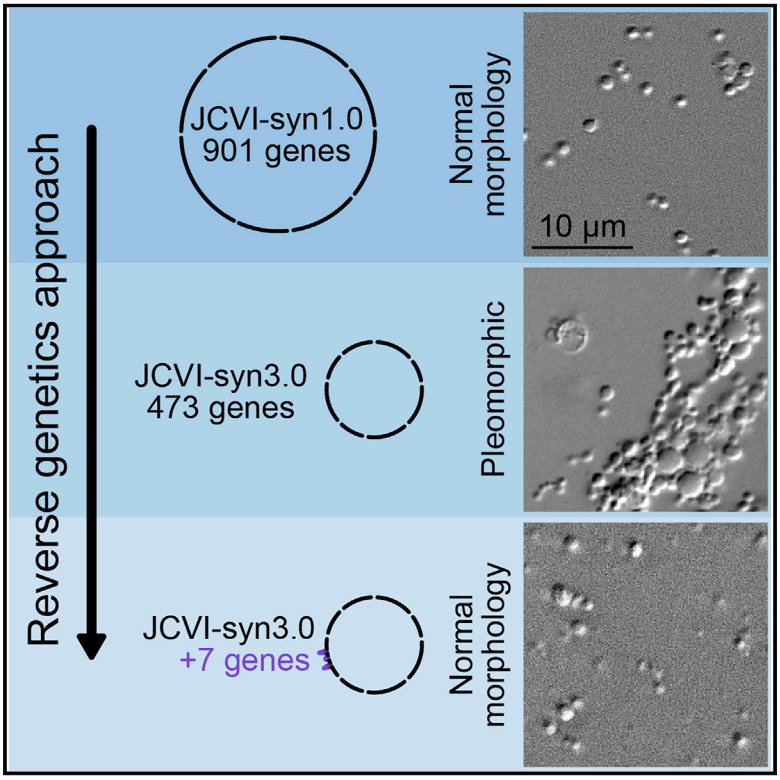

Highlights

- A reverse genetics approach determines genes required for normal cell division
- Normal cell division requires genes of known and unknown function
- JCVI-syn3A offers a genomically minimal model for bacterial physiology

Authors

James F. Pelletier, Lijie Sun, Kim S. Wise, ..., Ray-Yuan Chuang, John I. Glass, Elizabeth A. Strychalski

Correspondence

elizabeth.strychalski@nist.gov (E.A.S.), jglass@jcvi.org (J.I.G.)

In brief

A reverse genetics approach determined that seven genes are required together for normal cell division in a genomically minimal cell; these include two known cell division genes, *ftsZ* and *sepF*, a hydrolase of unknown substrate, and four genes that encode membrane-associated proteins of unknown function.

Pelletier et al., 2021, Cell *184*, 1–11
April 29, 2021 Published by Elsevier Inc.
https://doi.org/10.1016/j.cell.2021.03.008

Please cite this article in press as: Pelletier et al., Genetic requirements for cell division in a genomically minimal cell, Cell (2021), https://doi.org/10.1016/j.cell.2021.03.008

Cell

CellPress

Article

Genetic requirements for cell division in a genomically minimal cell

James F. Pelletier,[1,2,6] Lijie Sun,[3,6,7] Kim S. Wise,[3] Nacyra Assad-Garcia,[3] Bogumil J. Karas,[4] Thomas J. Deerinck,[5] Mark H. Ellisman,[5] Andreas Mershin,[1] Neil Gershenfeld,[1] Ray-Yuan Chuang,[3,8] John I. Glass,[3,*] and Elizabeth A. Strychalski[2,9,*]

[1]Center for Bits and Atoms, Massachusetts Institute of Technology, Cambridge, MA 02139, USA
[2]National Institute of Standards and Technology, Gaithersburg, MD 20899, USA
[3]J. Craig Venter Institute, La Jolla, CA 92037, USA
[4]Department of Biochemistry, Schulich School of Medicine and Dentistry, The University of Western Ontario, London, ON N6A 5C1, Canada
[5]National Center for Microscopy and Imaging Research, University of California-San Diego, La Jolla, CA 92037, USA
[6]These authors contributed equally
[7]Present address: Sorrento Therapeutics, Inc., San Diego, CA 92121, USA
[8]Present address: American Type Culture Collection, Manassas, VA 20110, USA
[9]Lead contact
*Correspondence: jglass@jcvi.org (J.I.G.), elizabeth.strychalski@nist.gov (E.A.S.)
https://doi.org/10.1016/j.cell.2021.03.008

SUMMARY

Genomically minimal cells, such as JCVI-syn3.0, offer a platform to clarify genes underlying core physiological processes. Although this minimal cell includes genes essential for population growth, the physiology of its single cells remained uncharacterized. To investigate striking morphological variation in JCVI-syn3.0 cells, we present an approach to characterize cell propagation and determine genes affecting cell morphology. Microfluidic chemostats allowed observation of intrinsic cell dynamics that result in irregular morphologies. A genome with 19 genes not retained in JCVI-syn3.0 generated JCVI-syn3A, which presents morphology similar to that of JCVI-syn1.0. We further identified seven of these 19 genes, including two known cell division genes, *ftsZ* and *sepF,* a hydrolase of unknown substrate, and four genes that encode membrane-associated proteins of unknown function, which are required together to restore a phenotype similar to that of JCVI-syn1.0. This result emphasizes the polygenic nature of cell division and morphology in a genomically minimal cell.

INTRODUCTION

Synthetic and engineering biology are creating new capabilities to investigate and leverage fundamental biological processes, for example, from sensors programmed as genetic circuits enabling control (Chen et al., 2020; Nielsen et al., 2016), to organisms with wholly recoded genomes (Annaluru et al., 2014; Fredens et al., 2019; Ostrov et al., 2016), to synthetic cells constructed from non-living parts (Hürtgen et al., 2019; Noireaux and Liu, 2020). Genome minimization offers a compelling synthetic biology approach to study the emergence of fundamental physiological processes from interactions between essential genes. Toward this goal, researchers at the J. Craig Venter Institute (JCVI) and collaborators applied genome minimization and an engineering biology workflow to develop a tractable platform for unicellular life that reflects known organisms and comprises the simplest free-living system. They accomplished this by building a functional synthetic genome that drives the propagation of a free-living cell (JCVI-syn1.0, nearly wild-type *Mycoplasma mycoides* subspecies *capri*) (Gibson et al., 2010) and subsequently reducing genome complexity to deliver a nearly minimal living bacterium, JCVI-syn3.0 (Figures 1A–1C; Hutchison et al., 2016). Genome minimization leveraged an engineering design-build-test-learn workflow based on the evaluation and combinatorial assembly of modular genomic segments, as well as empirical results obtained from transposon mutagenesis, to inform gene deletions. This approach both reduced bias in identifying essential genes and provided tools to alter, rebuild, and investigate the genome and encoded functions. With a reduction from 901 genes in JCVI-syn1.0 to 473 genes, the resulting strain JCVI-syn3.0 boasts the smallest genome of any free-living organism; yet, 149 of these essential genes are classified as genes of unknown or generic function. Many of these genes are conserved in walled bacteria, from which mycoplasmas evolved through massive gene loss. Mycoplasmas, such as JCVI-syn1.0 and JCVI-syn3.0, thus offer enabling platforms to probe essential processes conserved broadly in cellular life, as demonstrated here.

JCVI-syn3.0 grows axenically in a complex liquid medium that provides many nutrients the cell cannot synthesize, similar

Please cite this article in press as: Pelletier et al., Genetic requirements for cell division in a genomically minimal cell, Cell (2021), https://doi.org/10.1016/j.cell.2021.03.008

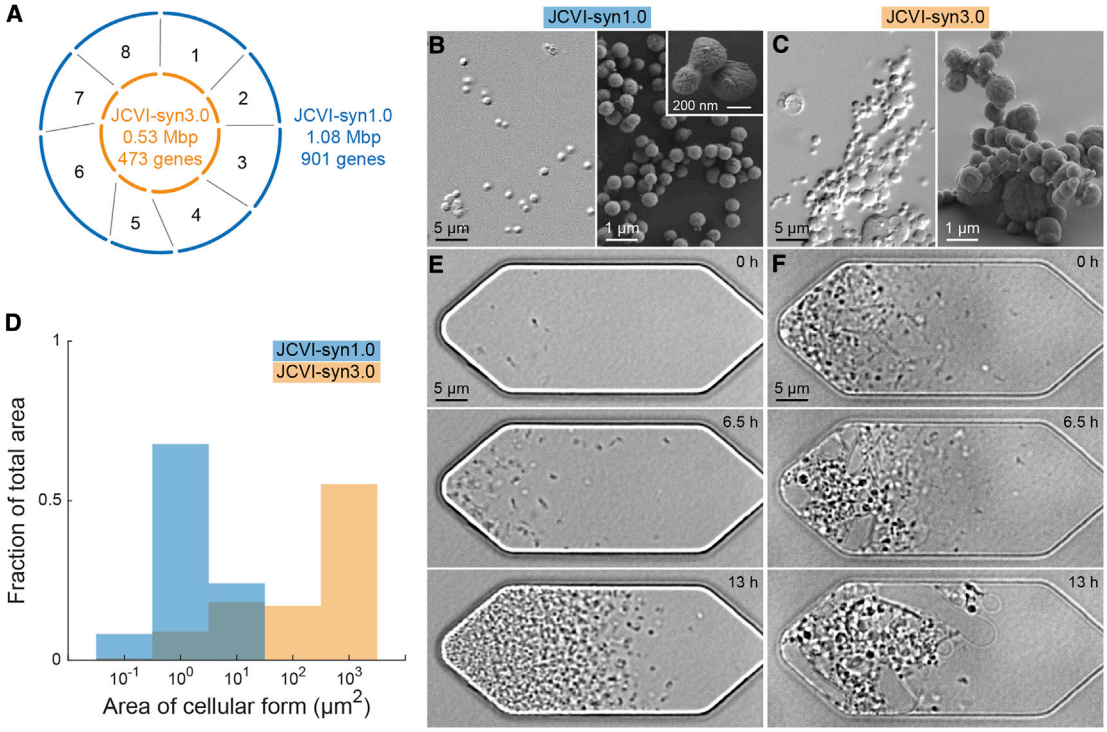

Figure 1. Genome reduction resulted in morphological variation at the cellular scale

(A) JCVI-syn3.0 is a genomically minimized cell derived from JCVI-syn1.0, which is similar to wild-type *M. mycoides*. Each genomic segment was minimized independently and then reassembled to produce the minimal JCVI-syn3.0 genome.

(B and C) Representative optical and scanning electron micrographs of cells grown in bulk liquid culture show (B) JCVI-syn1.0 with submicrometer, round cells of uniform size and shape and (C) JCVI-syn3.0 with variable size and shape. Some JCVI-syn3.0 cells appeared similar to JCVI-syn1.0 cells, whereas others clustered together or included large cellular forms with diameters $\geq$10 µm or irregular shapes.

(D) Frequency histograms of the area of each cell or cellular form show clear differences in the overall morphological variation of these strains at the cellular scale.

(E and F) Time-lapse optical micrographs of cell culture in microfluidic chemostats revealed the dynamic propagation of normal JCVI-syn1.0 cells and pleomorphic JCVI-syn3.0 cellular forms.

See also Figure S1 and Video S1.

to other mycoplasmas. A minimal replicative unit passes through a 0.22 µm filter and forms a typical mycoplasma colony. Moreover, measurements of cell-associated nucleic acid indicate logarithmic growth (Hutchison et al., 2016). The cell then meets two *sine qua non* of life: propagation of a membrane-bound compartment containing the genome with its replicative machinery and replication of that genome. Nevertheless, a wholly unexpected feature of JCVI-syn3.0 is the striking morphological variation of individual cells, with filamentous, vesicular, and other irregular forms described previously using static optical and scanning electron micrographs (Figure 1C; Hutchison et al., 2016). These morphologies are absent in both wild-type *M. mycoides* and JCVI-syn1.0 cells, which exhibit what we refer to here as "normal morphology" consisting of spherical cells $\approx$400 nm in diameter (Figure 1B; Hutchison et al., 2016).

To determine the genetic requirements for normal morphology and cell division in the genomically minimal context of JCVI-syn3.0, we pursued a reverse genetics approach informed by microfluidic imaging of cellular growth. Static images cannot reveal the biogenesis of pleomorphic cellular forms, their content, or their relevance in propagation. We report here on the propagation of membrane compartments and confirm these shapes arise from morphological dynamics intrinsic to individual cells via imaging in microfluidic chemostats. We then investigated the genetic requirements to restore normal morphology to pleomorphic strains through various, nearly minimal genomes. We identified a nearly minimal strain, JCVI-syn3A, which has 19 genes not retained in JCVI-syn3.0 and presents significantly less morphological variation than JCVI-syn3.0. JCVI-syn3A is mechanically robust to the liquid handling required for biological research and compatible with practical computational modeling of a minimal metabolism (Breuer et al., 2019). A reverse genetics approach subsequently determined that seven of the 19 genes, of known and unknown function, were necessary to restore normal morphology. The requirement for all seven genes, including *ftsZ*, *sepF,* a hydrolase of unknown substrate, and others encoding membrane-associated proteins of unknown function, highlights a role for FtsZ and membrane biophysics in the scission of genomically minimized cells.

Please cite this article in press as: Pelletier et al., Genetic requirements for cell division in a genomically minimal cell, Cell (2021), https://doi.org/10.1016/j.cell.2021.03.008

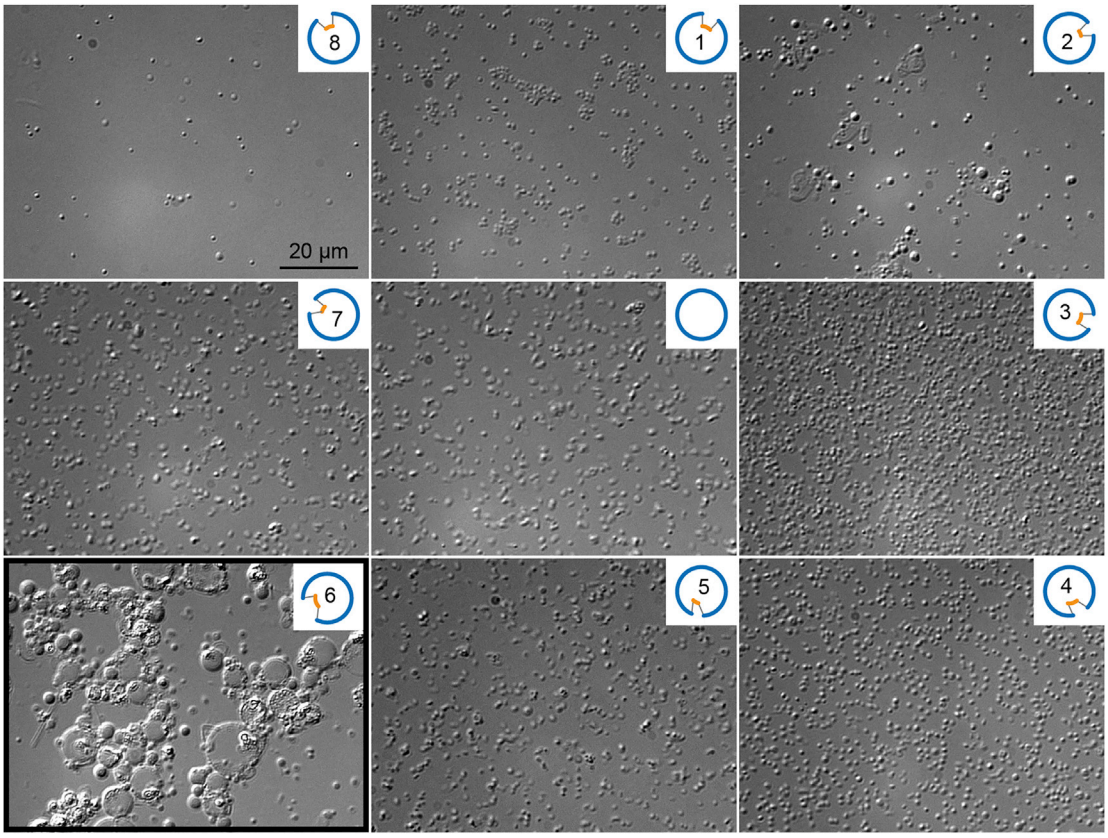

Figure 2. Genes in segment 6 strongly influenced morphological variation at the cellular scale

Tests of each minimized genomic segment (orange arcs) in the context of the JCVI-syn1.0 genome (blue circle) revealed that segment 6 generated pleomorphic cellular forms similar to JCVI-syn3.0. Samples were prepared and imaged as for Figures 1B and 1C.

RESULTS

Dynamic propagation of genomically minimized cells

To characterize the morphology of JCVI-syn3.0 and related genomically minimized strains at the cellular scale, we obtained time-lapse images in microfluidic chemostats (Figures 1E and 1F; Video S1). This platform shielded cells from shear flow, which can affect mycoplasmal morphology (Razin et al., 1967) and has been proposed to facilitate scission of primordial cells (Chen, 2009). Thus, the microfluidic chemostat isolated mechanisms of propagation and cell division intrinsic to a cell and revealed directly the emergence and dynamics of diverse morphologies (Figure S1; STAR Methods). Strains exhibited similar phenotypic variation in both static liquid culture and microfluidic chemostats.

Using these observations, we separated strains into two general morphological classes: normal and pleomorphic. JCVI-syn1.0 defined the normal morphology, with round, submicrometer cells, largely disconnected from one another (Figure 1B). In contrast, JCVI-syn3.0 exemplified pleomorphic morphologies, including large cellular forms with diameters $\geq$10 μm and irregular shapes (Figure 1C). We use the term "cellular form" to describe complex morphologies with adjacent substructures. Although some JCVI-syn3.0 cells appeared similar to JCVI-syn1.0 cells, the majority consisted of large cellular forms (Figure 1C). The area distribution of cells and cellular forms was quantified using static liquid culture (Figure 1D; STAR Methods), whereas the dynamics of propagation were observed in microfluidic chemostats (Figures 1E and 1F; Video S1). We apply the general term "propagation" to describe shape changes that accompany growth and reserve the term "cell division" for complete scission.

Morphological diversity from a single minimized genomic segment

To perform an unbiased screen for genes correlated with morphological variation, we exploited the segmented structure of the JCVI-syn3.0 genome. During the process of genome minimization from JCVI-syn1.0 to JCVI-syn3.0, genes or gene clusters were removed in various combinations from individual genomic segments. Each minimized segment in the context of an otherwise JCVI-syn1.0 genome showed viability and growth at the population scale (Hutchison et al., 2016). Re-examining these strains here at the cellular scale, we noted one strain, termed RGD6 (reduced genome design segment 6), contained the fully minimized genomic segment 6 and demonstrated striking pleomorphism similar to JCVI-syn3.0 (Figures 2, 3, and 4, cf. Figure 1C). Each of the other minimized segments in an

Please cite this article in press as: Pelletier et al., Genetic requirements for cell division in a genomically minimal cell, Cell (2021), https://doi.org/10.1016/j.cell.2021.03.008

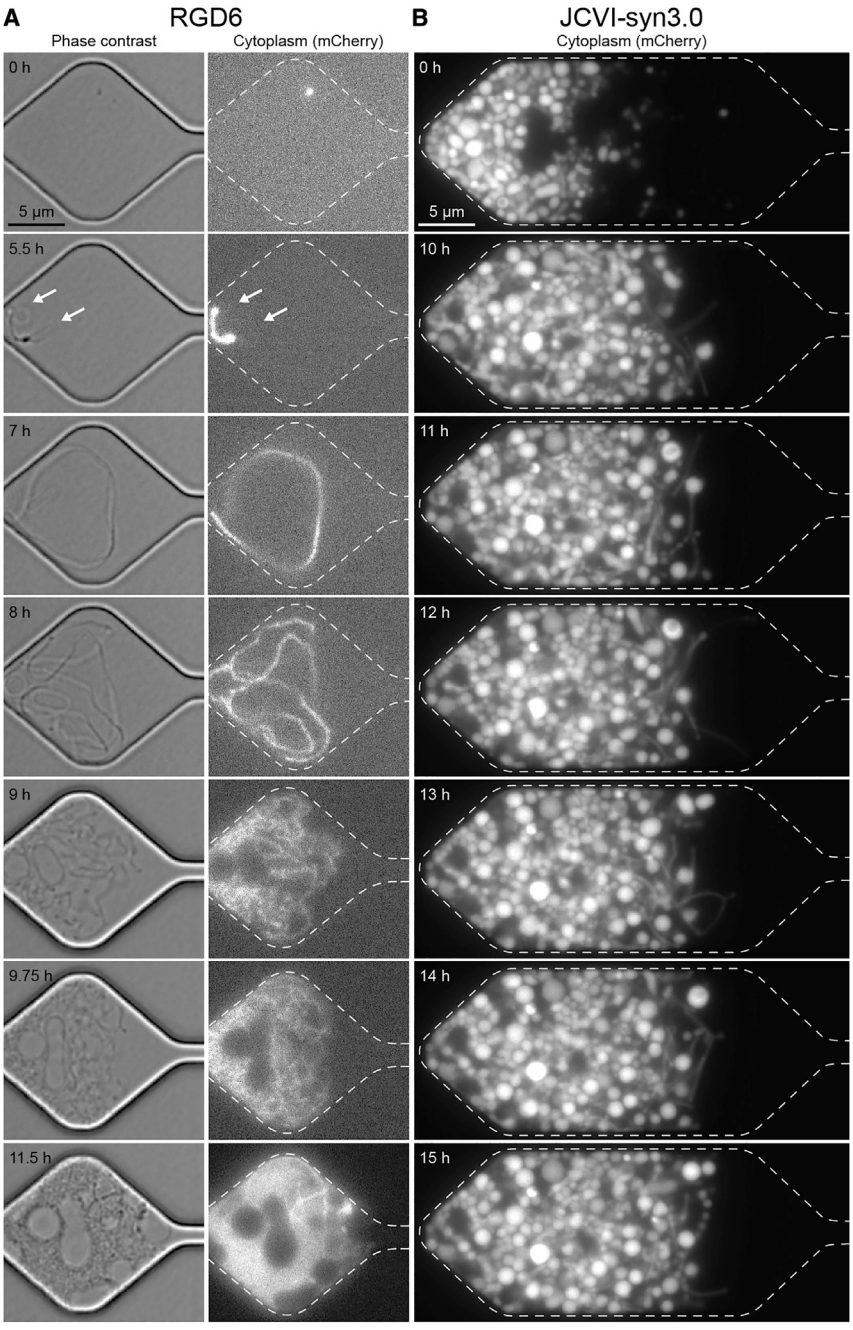

Figure 3. RGD6 and JCVI-syn3.0 exhibited filamentation, branching, pearling, and other morphological dynamics in the absence of shear flow

(A) RGD6 was capable of filamentous propagation in the shear-free environment of microfluidic chemostats. Left column: phase contrast images. Right column: constitutively expressed mCherry as a marker for cytoplasm. Chemostat walls are indicated as dotted lines. White arrows at 5.5 h indicate the appearance of vesicles, which lacked mCherry, at the ends of the filament.

(B) Growth of JCVI-syn3.0 produced pearled and branched filaments, along with other morphologies, shown here in a representative chemostat loaded with many cells at the start of the experiment.

See also Figure S1 and Videos S2 and S3.

otherwise JCVI-syn1.0 genome resulted in normal or nearly normal morphology (Figure 2).

The comparable growth rate of RGD6 to JCVI-syn1.0 facilitated experimental investigation of the propagation of pleomorphic cellular forms (Figure 3A; Video S2). JCVI-syn3.0 appeared similar to RGD6, including irregular and filamentous cellular forms, which exhibited branching or pearling, with round, connected substructures (Figure 3B; Video S3). In a representative microfluidic experiment, a single RGD6 propagated into a striking variety of morphologies (Figure 3A; Video S2). The small cell grew into a filamentous cellular form, and vesicles appeared at the ends (Figure 3A). The vesicles lacked observable mCherry, which serves as a marker for cytoplasmic protein, from their first appearance. The filamentous cellular form increased in length and bent to fit within the chamber, while the vesicles continued to grow. Note that not all RGD6 cells showed filamentous propagation (cf. Figures 2 and 4E).

To probe the internal structure of pleomorphic cellular forms, fluorescence imaging informed cellular composition and organization. We visualized cytoplasm with constitutively expressed fluorescent mCherry protein, nucleoids with Hoechst 33342 stain, membranes with the lipophilic dye SP-DiOC18(3), and extracellular growth medium with fluorophore-conjugated dextran (Figure S1). Filamentous cellular forms contained mCherry and often appeared with multiple nucleoids along their length, suggesting genome replication and segregation continued in the absence of complete scission. Although vesicles generally did not contain observable mCherry, they were labeled by the membrane dye and excluded fluorescent dextran from their interiors (Figure S1). This finding suggests that vesicles lacked cellular machinery needed for mCherry expression but remained bounded by membranes impermeable to macromolecules.

Genomic restoration of normal morphology in a nearly minimal cell

To determine the genes in segment 6 required for normal division, we leveraged genetics approaches enabled by the synthetic, modular, and minimal aspects of the genome. In particular, we pursued a systematic, reverse genetics approach, testing the dependence of morphological variation first on gene clusters

Please cite this article in press as: Pelletier et al., Genetic requirements for cell division in a genomically minimal cell, Cell (2021), https://doi.org/10.1016/j.cell.2021.03.008

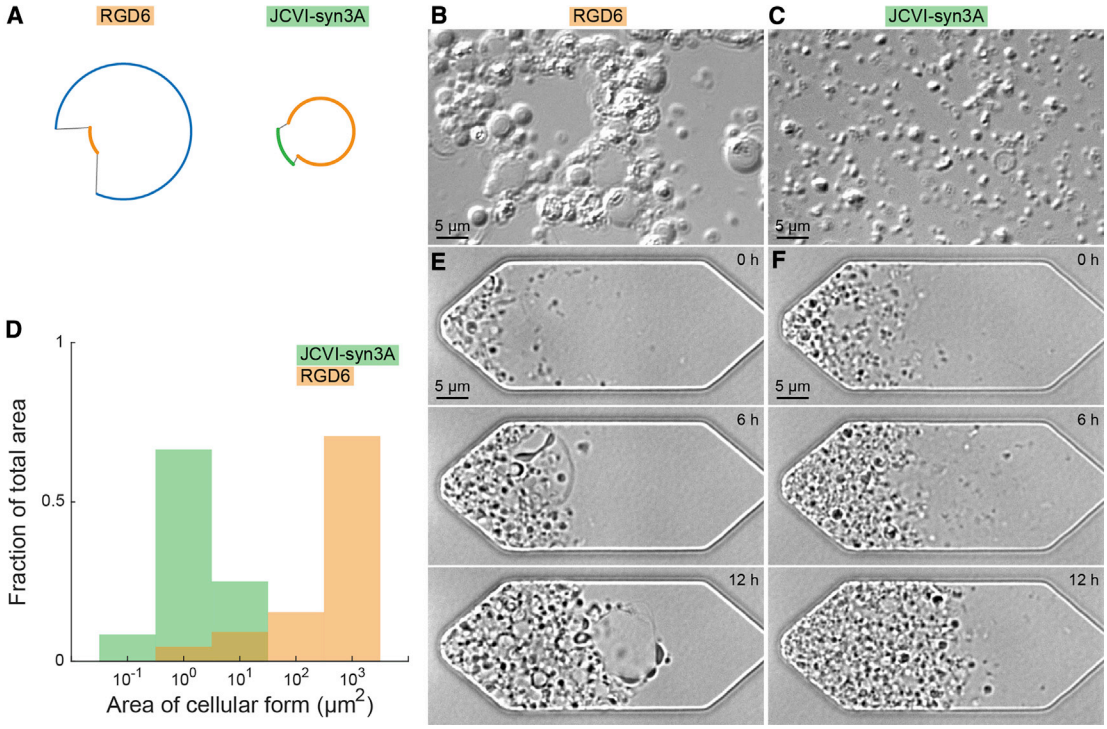

Figure 4. A genome with 19 genes not retained in JCVI-syn3.0 significantly reduced morphological variation

(A) RGD6 includes the minimized segment 6 from JCVI-syn3.0, while JCVI-syn3A has a nearly minimal segment 6 containing 19 additional genes.

(B and C) Optical micrographs show cells grown in bulk liquid culture.

(B) RGD6 produced dramatic morphological variation similar to JCVI-syn3.0.

(C) In contrast, JCVI-syn3A exhibited significantly less morphological variation, similar to JCVI-syn1.0.

(D–F) The growth of JCVI-syn3A in the microfluidic chemostat appeared similar to JCVI-syn1.0 (Figure 1E). The significant reduction in morphological variation between RGD6 and JCVI-syn3A is evident by comparing (B and C) optical micrographs, (D) the frequency histograms of the area of cellular forms, and (E and F) growth in microfluidic chemostats.

See also Figure S1 and Video S4.

and subsequently on individual genes in segment 6 (Figure S2). Among the 76 genes removed from segment 6 to generate JCVI-syn3.0 was an *ftsZ*-containing cluster (genes *520–522*), which lay within the *dcw* locus, a conserved cluster of genes known to participate in programmed cell division in most bacteria (Alarcón et al., 2007; Benders et al., 2005; Eraso et al., 2014; Vedyaykin et al., 2019). One nearly minimal version of segment 6 retained this *ftsZ*-containing cluster, along with genes outside the *dcw* cluster. This segment conferred a nearly normal morphology when replacing the minimized segment 6 in JCVI-syn3.0, thereby creating a strain JCVI-syn3A (Figure 4; Video S4). The <2 h doubling time of JCVI-syn3A is reduced from that of JCVI-syn3.0 (Breuer et al., 2019). The fully annotated genome sequence of JCVI-syn3A is deposited in NCBI (GenBank: CP016816.2).

Segment 6 in JCVI-syn3A contains 19 genes not present in the fully minimized version of JCVI-syn3.0 (Figure 5). We proceeded to identify the genes required for normal morphology by adding subsets of these 19 genes to JCVI-syn3.0. Three of these genes represent a redundant copy of the rRNA operon, which we determined here to not affect morphology. The remaining 16 genes encoding proteins were grouped in eight clusters of contiguous genes (Figure 5A). In principle, clusters could represent single transcriptional units. To account for this, we introduced clusters of contiguous genes into JCVI-syn3.0, followed by deleting individual genes. Genes or gene clusters were reintroduced at ectopic loci and included adjoining sequence to retain native regulatory regions (Hutchison et al., 2016). These precautions allowed us to evaluate whether the presence of a gene or cluster, even outside its native locus, was sufficient to confer the normal phenotype.

We hypothesized that addition of the *ftsZ*-containing cluster would restore normal cell division and would alone confer the same reduction in morphological variation as observed in JCVI-syn3A. The *ftsZ*-containing cluster comprises three genes—*ftsZ*, *sepF*, and an adjacent hydrolase of unknown substrate. Although part of the highly conserved division and cell wall (*dcw*) cluster present in the original JCVI-syn1.0 (Figure 5B), this subcluster was removed during genome minimization. Adding the *ftsZ*-containing cluster alone was not sufficient to reduce morphological variation in JCVI-syn3.0 (Figures 5C and 5D), whereas JCVI-syn3A retained a nearly normal morphology upon deletion of the *ftsZ*-containing cluster (Figure S3). The complex genetic basis for this phenotype required that we apply a more systematic approach to identify genes necessary and sufficient to restore a more normal phenotype in the genomic context of JCVI-syn3.0.

Please cite this article in press as: Pelletier et al., Genetic requirements for cell division in a genomically minimal cell, Cell (2021), https://doi.org/10.1016/j.cell.2021.03.008

A

Additional genes in JCVI-syn3A

Necessary for normal morphology | Not necessary for normal morphology

Gene cluster	Locus tag	Annotation	Functional category
1	*520*	Alpha/beta hydrolase superfamily	Unknown
	521	SepF	Cell division
	522	FtsZ	Cell division
2	*527*	Protein of unknown function, DUF177 domain	Unknown
	532	5S (*rrf*) ribosomal RNA, Second copy	rRNA
	533	23S (*rrl*) ribosomal RNA, Second copy	rRNA
	534	16S (*rrs*) ribosomal RNA, Second copy	rRNA
3	*538*	Protein of unknown function	Unknown
4	*546*	Sucrose-6F-phosphate phosphohydrolase domain	Carbon metabolism
	548	Putative tRNA (cytidine(34)-2'-O)-methyltransferase	rRNA modification
	549	Non-canonical purine NTP pyrophosphatase, RdgB/HAM family	Nucleotide salvage
5	*592*	PF09903 family	Unknown
	593	Protein of unknown function	Unknown
6	*602*	Protein of unknown function	Unknown
	604	LemA/GacS family	Unknown
	605	Protein of unknown function	Unknown
7	*610*	MutM, DNA-formamidopyrimidine glycosylase	DNA repair
8	*622*	Putative lipoprotein	Lipoprotein
	623	Protein of unknown function	Unknown

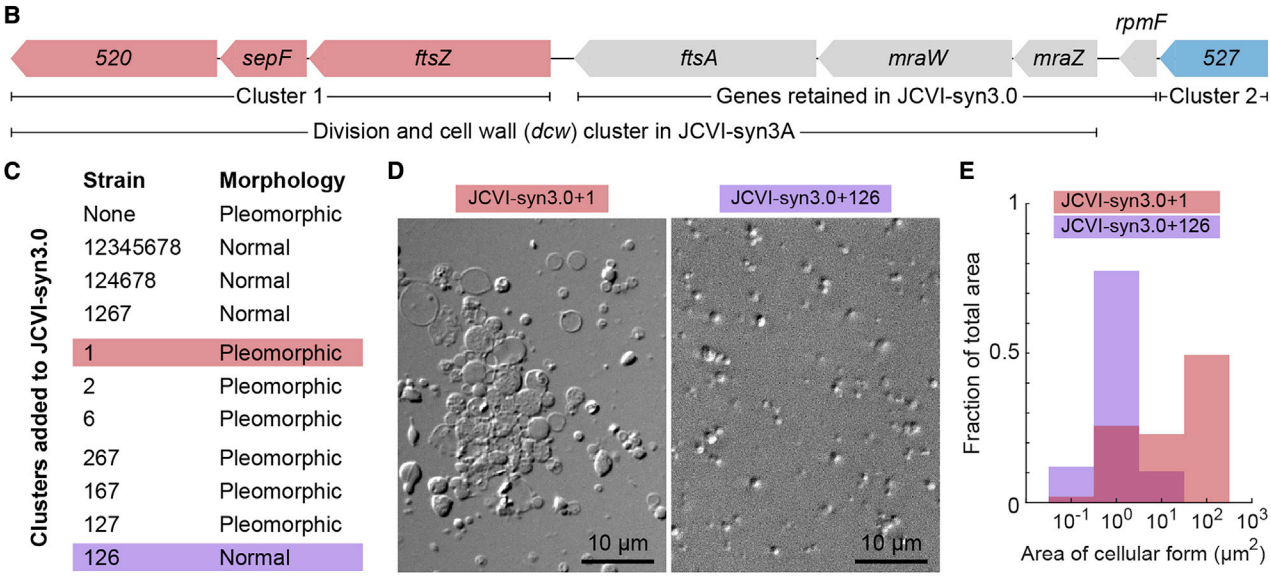

Figure 5. Seven of the 19 additional genes in JCVI-syn3A restored normal morphology to JCVI-syn3.0

(A) 19 genes in JCVI-syn3A are not retained in JCVI-syn3.0 and occurred in clusters of single or contiguous genes. One cluster represents a second copy of an rRNA operon. The other eight clusters encode proteins.

(B) The *ftsZ*-containing cluster 1 is contained within a highly conserved division and cell wall (*dcw*) cluster in JCVI-syn3A, part of which is retained in JCVI-syn3.0. Arrows indicate gene direction, and black lines between genes indicate intergenic sequences.

(C) The addition of cluster 1 alone was insufficient to restore normal morphology, whereas clusters 1, 2, and 6 together, which include genes of unknown function, recovered the normal phenotype.

(D) Optical micrographs show the pleomorphism of JCVI-syn3.0+1 and the normal morphology of JCVI-syn3.0+126.

(E) Area distributions of cellular forms confirm these morphological classifications.

See also Figures S3, S4, and S5 and Table S1.

Please cite this article in press as: Pelletier et al., Genetic requirements for cell division in a genomically minimal cell, Cell (2021), https://doi.org/10.1016/j.cell.2021.03.008

We validated our approach of inserting genes at ectopic loci by adding all eight clusters to the JCVI-syn3.0 genome and confirmed restoration of normal morphology (Figure 5C, strain JCVI-syn3.0+12345678). This strain had the same gene content as JCVI-syn3A without the redundant rRNA operon, thereby confirming this second rRNA operon was unnecessary for the normal phenotype. By including fewer clusters, we arrived at strain JCVI-syn3.0+1267 with normal morphology. Based on this strain, normal morphology did not require the omitted clusters 3, 4, 5, and 8. The addition of clusters individually to JCVI-syn3.0 resulted in pleomorphic strains, indicating each cluster alone was insufficient to restore the normal phenotype. We finally attempted to omit each cluster separately from JCVI-syn3.0+1267. Although cluster 7 was dispensable, all others were necessary to restore normal morphology (Figure S4).

Having determined all necessary clusters, we tested each remaining gene individually. We employed the strain JCVI-syn3.0+126 (Figure 5D), which resembles the phenotype of JCVI-syn3A (Figure 4C), as a genomic framework and deleted each of the seven genes (Figure S5). These included the three genes in the *ftsZ*-containing cluster, as well as the four genes of unknown function outside this locus. Gene coding regions were deleted in-frame to preserve transcriptional and translational integrity for genes within possible operons. None of the seven genes could be removed without reverting to the pleomorphic phenotype of JCVI-syn3.0 (Figure S5; Table S1). This provides strong evidence that all seven genes were necessary and together sufficient to reduce morphological variation in JCVI-syn3.0 to that of JCVI-syn3A (Figures 5D and 5E).

DISCUSSION

Morphological dynamics intrinsic to cells revealed by microfluidic chemostats

As mycoplasmas lack a peptidoglycan cell wall, mycoplasmal morphologies are sensitive to shear flow, which can drive filamentation (Razin et al., 1967). Here, the microfluidic chemostat sheltered cells from shear flow, while enabling observation of their growth and propagation and ensuring that filamentous and other forms reflected morphological dynamics intrinsic to cells. In striking contrast to JCVI-syn1.0, our study suggests that JCVI-syn3.0 lost the ability to control cell division. This is seen perhaps most clearly in the marked diversity of these cellular forms emerging from a single replicative unit. It was unknown how JCVI-syn3.0 propagated in the absence of controlled cell division, as in JCVI-syn1.0. We observed that genomically minimized strains displayed a wide variety of dynamics (Figures 1F, 3, and 4E; Videos S1, S2, S3, and S4). Filamentous growth was notable, in particular, given the lack of a cell wall or bacterial cytoskeletal elements to generate and stabilize these cellular forms. Although some filaments exhibited branching or pearling, we did not observe scission, consistent with the presence of an energy barrier (Beltrán-Heredia et al., 2017; Caspi and Dekker, 2014; Ruiz-Herrero et al., 2019).

These growth characteristics appeared similar to L-form bacteria, which are variants that lack their typical cell wall (Errington, 2017). Mycoplasmas and L-forms have long been compared to one another, because both lack a cell wall and appear similar in optical (Kang and Casida, 1967) and electron micrographs (Dienes and Bullivant, 1968). Given these morphological similarities, genomically minimized mycoplasmas and L-forms may share common mechanisms of propagation. In particular, some L-forms undergo an irregular cell division mechanism, termed "extrusion-resolution," involving extrusion of excess membrane, followed by resolution of the extrusion into connected units (Errington, 2017). This mechanism requires excess membrane synthesis (Mercier et al., 2013), does not require FtsZ or FtsA (Leaver et al., 2009), and is suppressed by confinement in submicrometer microfluidic channels (Wu et al., 2020). Our observations suggest the extrusion-resolution model is relevant to propagation of JCVI-syn3.0 and related genomically minimized strains, and our study highlights a wide range of morphological dynamics that can occur without shear flow.

Systematic approach attributes morphology to genes of unknown function

We applied a reverse genetics approach—first screening multiple variants of genome segments, followed by gene clusters, and finally individual genes—to determine a set of seven genes, all of which were required together to recover normal morphology in the genomically minimal context of JCVI-syn3.0. This systematic approach enabled the identification of proteins with previously unknown function as necessary for normal morphology in the minimal cell. Although their functions remain unclear, genes *527* and *604* are expressed abundantly in JCVI-syn3A, with several hundred copies per cell, whereas genes *520*, *521*, and *605* were detected in lower quantities (Breuer et al., 2019). Furthermore, some protein sequence motifs are highly conserved across bacterial species. Gene *527* is homologous to the DUF177 family, which may participate in biosynthesis of membrane-associated proteins (Yang et al., 2016), whereas gene *604* is homologous to LemA/GacS, a family of two-component regulatory proteins (Hrabak and Willis, 1992). Two-component regulatory systems have not been reported in mycoplasmas (Capra and Laub, 2012), nor are any two-component genes other than the *lemA/gacS* gene observed here, leaving the function of gene *604* unclear in both JCVI-syn3A and JCVI-syn3.0+126. Analysis of secondary structure revealed membrane association of proteins encoded by genes *604* and *605*, which include one transmembrane helix and a bacterial lipoprotein anchoring motif, respectively. Gene *602* is annotated as a pseudogene, due to a confirmed frameshift mutation causing truncation relative to full-length orthologs in the *Mycoplasma mycoides* group. The N-terminal portion, predicted to be expressed, contains two transmembrane helices. Therefore, although these four genes outside the *dcw* cluster lack known function, bioinformatic analyses indicate they associate with the membrane, suggesting unknown roles for membrane properties in cell division and morphology.

Requirement for FtsZ for normal cell division depends on genomic context

Despite extensive characterization of the multicomponent systems underlying cell division in walled bacteria, a full understanding of cell propagation in those organisms is far from complete (Margolin, 2020; Osawa and Erickson, 2018). Gaps in

Please cite this article in press as: Pelletier et al., Genetic requirements for cell division in a genomically minimal cell, Cell (2021), https://doi.org/10.1016/j.cell.2021.03.008

understanding include spatiotemporal control and interactions among the myriad proteins involved, as well as mechanisms of force transduction. In phylogenetically related mycoplasmas in the *M. mycoides* group, only incomplete models of cell division have been reported (Seto and Miyata, 1998). As a framework to simplify and study genetic requirements of cell division and morphological control, JCVI-syn3A and JCVI-syn3.0+126 present compelling platforms, because they lack most cell division components of walled bacteria and many alterations to the genotype resulted in readily observable phenotypic variation.

Normal cell division required the *ftsZ*-containing cluster in JCVI-syn3.0+126. This strain retains FtsA and SepF, which can anchor FtsZ to the membrane (Duman et al., 2013; Hamoen et al., 2006; Loose and Mitchison, 2014), as well as modulate the assembly and bundling of FtsZ (Krupka and Margolin, 2018; Singh et al., 2008). FtsA can polymerize *in vitro* (Szwedziak et al., 2012), but the proteome of JCVI-syn3A includes only ≈40 copies per cell—significantly less than FtsZ at ≈640 copies per cell (Breuer et al., 2019). In both *Escherichia coli* and *Bacillus subtilis*, cell division occurs when FtsZ accumulates to a threshold number per cell, although its molecular mechanism and interactions with other proteins remain unclear (Sekar et al., 2018; Si et al., 2019). JCVI-syn3.0 retains other *dcw* cluster genes, *mraZ* and *mraW*, but MraZ was not detected in the JCVI-syn3A proteome (Breuer et al., 2019). JCVI-syn3.0+126 also lacks genes known to facilitate aspects of FtsZ function, such as degradation and positioning. Purified FtsZ protofilaments are intrinsically curved (Housman et al., 2016); we speculate that alignment of FtsZ along maximal membrane curvature may help localize FtsZ to the division furrow, similar to the orientation of another intrinsically curved filament, MreB, along the maximal membrane curvature in *B. subtilis* (Hussain et al., 2018).

Normal cell division did not require the *ftsZ*-containing cluster in JCVI-syn3A. The disparate genomic context between JCVI-syn3A and JCVI-syn3.0+126 may contribute to differing requirements for FtsZ in these strains. For example, JCVI-syn3A contains 12 additional genes relative to JCVI-syn3.0+126, including a duplicate rRNA operon (Figure 5A). Transcriptional context may also vary between these strains. In particular, the seven genes identified by our reverse genetics approach were expressed from native loci in JCVI-syn3A but ectopic loci in JCVI-syn3.0+126. Regardless of genomic and transcriptional contexts, normal morphology and division required the four genes encoding membrane-associated proteins of unknown function in both JCVI-syn3.0 and JCVI-syn3A (Table S1).

Minimal cells highlight membrane biophysics in cell division

The normal morphology of some strains lacking FtsZ, as well as the requirement for genes of unknown function, indicates other processes contribute to morphological control. Our results from both imaging and genetics experiments indicate the influence of membrane properties on cell morphology. In microfluidic chemostats, JCVI-syn3.0 and RGD6 displayed aberrant membrane-bound vesicles, consistent with dysregulation of membrane accumulation linked with pleomorphism. Bioinformatic analyses suggest membrane association of the products of the four required genes of unknown function outside the *dcw* cluster. Maintenance of membrane homeostasis is critical in cellular organisms, including bacteria (Ernst et al., 2016; Zhang and Rock, 2008), but is not well understood in mycoplasmas, which have adapted through evolution to acquire membrane components directly from the environment (Breuer et al., 2019). Membrane components from the environment can affect mycoplasmal morphology. For example, the lipid composition of the growth medium affects whether mycoplasmas phylogenetically similar to JCVI-syn1.0 form spherical cells or filaments (Razin et al., 1967). Furthermore, cell division requires membrane synthesis in mycoplasmas phylogenetically similar to JCVI-syn1.0 (Seto and Miyata, 1999). Theories and observations of abiotic vesicles predict a wide range of morphological dynamics similar to those observed here, including spontaneous filamentation and pearling (Caspi and Dekker, 2014; Lipowsky, 2013), which depend on membrane properties, such as spontaneous curvature, elastic modulus, and fluidity. With defined, nearly minimal genomes and an experimental niche that can be manipulated to deliver lipids, JCVI-syn3A and JCVI-syn3.0+126 present ideal model systems for examining the role of membrane dynamics in cellular propagation.

Conclusions

We present the first use of genomically minimized cells to determine the genetic requirements for the core physiological processes of cell division and the maintenance of cell morphology. Starting with the minimal cell JCVI-syn3.0, which shows irregular cell division and pleomorphism, we reconstituted a set of genes that conferred nearly normal division and morphology. The resulting strains, JCVI-syn3A and JCVI-syn3.0+126, have nearly minimal genomes and metabolism, as well as cell morphology typical of JCVI-syn1.0 and most spherical bacteria. These strains thus offer compelling minimal models for bacterial physiology and platforms for engineering biology broadly. Of the 19 additional genes present in JCVI-syn3A, seven were required and together sufficient to restore a more normal phenotype to JCVI-syn3.0. Five of these genes have no known function. Our systematic approach, agnostic to gene function, discovered their requirement for normal cell division and morphology and may find application to organisms beyond mycoplasmas. The role of these previously uncharacterized genes, as well as the polygenic basis of normal cell division and morphology, will inform bottom-up approaches to reconstitute cell division in synthetic cells.

Limitations of study

Our microfluidics approach allowed observation of the intrinsic dynamics of pleomorphic cellular forms. Their small size and diffusion within the microfluidic chemostats complicated our ability to resolve single cells for straightforward image analysis. The chemostat environment, which relies on diffusive exchange, requires further characterization during cell propagation. Future studies of cell physiology could involve optical imaging techniques with higher spatial resolution, improved fluidic confinement, methods to mitigate phototoxicity, and more quantitative analysis of morphology and cellular composition throughout the cell cycle.

We designed this study to determine the genetic requirements for normal morphology and cell division in a genomically minimal cell. Although this allowed assignment of seven genes of known and previously unknown function to cell division and possibly to membrane accumulation, the study was neither intended nor able to identify specific biochemical, metabolic, or structural functions associated with individual gene products. A combination of experimental approaches may elucidate these functions in future studies. Although the seven genes we identified are conserved widely in most bacteria, some pleomorphic bacteria lack most of these genes. Comparative genomics analyses focused on the seven genes could inform generally on these processes in bacterial physiology.

Mycoplasmas evolved to acquire nutrients from multicellular eukaryotes and grow axenically in the laboratory on a rich growth medium containing complex, not fully defined, and potentially variable additives. This study therefore used a consistent growth medium throughout. The dependence of these cells on externally supplied lipids, as well as the potential role of lipids in determining membrane properties that may influence propagation, underscores the need for additional studies and optimization in a defined growth medium. Characterizing and controlling the external environment, including the growth medium, will also advance whole cell modeling of a minimal cell.

STAR★METHODS

Detailed methods are provided in the online version of this paper and include the following:

- KEY RESOURCES TABLE
- RESOURCE AVAILABILITY
  - Lead contact
  - Materials availability
  - Data and code availability
- EXPERIMENTAL MODEL AND SUBJECT DETAILS
  - Bacterial strains and growth media
- METHOD DETAILS
  - Microscopy of bulk cultures
  - Scanning electron imaging
  - Microfluidic platform fabrication
  - Microfluidic cell culture and imaging
  - Genome synthesis and assembly
  - Construction of genomes by combining segments
  - Gene additions to JCVI-syn3.0
  - Transformation of JCVI-syn3.0 using plasmids
  - Construction of plasmids
  - Insertion of mCherry into genomes
  - Yeast assembly of plasmids
  - Guide RNA production and quantification
  - CRISPR donor DNA preparation
  - Yeast transformation and screening
  - Genome transplantation
  - Gene removal from bacterial genomes in yeast
  - Deletion of one gene cluster from JCVI-syn3.0+1267
  - Deletion of genes from JCVI-syn3.0+126 using CRISPR/Cas9
- QUANTIFICATION AND STATISTICAL ANALYSIS
  - Empirical gradient thresholding to estimate cell size distributions

SUPPLEMENTAL INFORMATION

Supplemental information can be found online at https://doi.org/10.1016/j.cell.2021.03.008.

ACKNOWLEDGMENTS

The authors thank Daniel Dwyer, Nikta Fakhri, Christine Field, Clyde Hutchison, Suckjoon Jun, Thomas Knight, Timothy Mitchison, Hamilton Smith, and Shuguang Zhang for critical feedback and helpful conversations. J.F.P. was supported by a Fannie and John Hertz Foundation Fellowship, the Mitchison lab at Harvard Medical School, and the Fakhri lab at MIT. E.A.S. was supported by the National Institute of Standards and Technology (certain commercial equipment, instruments, or materials are identified in this paper to foster understanding; such identification does not imply recommendation or endorsement by the National Institute of Standards and Technology, nor does it imply that the materials or equipment identified are necessarily the best available for the stated purpose). L.S., K.S.W., and J.I.G. were supported by the National Science Foundation (MCB 1840320 and MCB 1818344 to J.I.G.). L.S., K.S.W., N.A.-G., B.J.K., R.-Y.C., and J.I.G. were supported by Synthetic Genomics, Inc., the Defense Advanced Research Projects Agency's Living Foundries program (HR0011-12-C-0063), and the J. Craig Venter Institute. Microscopy work at the University of California-San Diego was supported by NIH grant P41GM103412 from the National Institute of General Medical Sciences to M.H.E.

AUTHOR CONTRIBUTIONS

J.F.P., L.S., K.S.W., J.I.G., and E.A.S. authored the manuscript. J.F.P. and E.A.S. fabricated the microfluidic chemostats and performed microfluidic measurements. L.S. performed experiments to reintroduce genes and identify those which result in improved morphological uniformity of JCVI-syn3.0. L.S. and K.S.W. provided optical microscopy of wet mounts. L.S., N.A.-G., B.J.K., and R.-Y.C. generated the bacterial strains. T.J.D. and M.H.E. performed electron microscopy. A.M. and N.G. assisted in developing the microfluidic chemostat and its operation.

DECLARATION OF INTERESTS

The authors declare no competing interests.

Received: January 25, 2018
Revised: January 27, 2021
Accepted: March 3, 2021
Published: March 29, 2021

REFERENCES

Alarcón, F., Vasconcelos, A.T.R.d., Yim, L., and Zaha, A. (2007). Genes involved in cell division in mycoplasmas. Genet. Mol. Biol. *30*, 174–181.

Annaluru, N., Muller, H., Mitchell, L.A., Ramalingam, S., Stracquadanio, G., Richardson, S.M., Dymond, J.S., Kuang, Z., Scheifele, L.Z., Cooper, E.M., et al. (2014). Total synthesis of a functional designer eukaryotic chromosome. Science *344*, 55–58.

Beltrán-Heredia, E., Almendro-Vedia, V.G., Monroy, F., and Cao, F.J. (2017). Modeling the mechanics of cell division: Influence of spontaneous membrane curvature, surface tension, and osmotic pressure. Front. Physiol. *8*, 312.

Benders, G.A., Powell, B.C., and Hutchison, C.A., 3rd. (2005). Transcriptional analysis of the conserved *ftsZ* gene cluster in *Mycoplasma genitalium* and *Mycoplasma pneumoniae*. J. Bacteriol. *187*, 4542–4551.

Breuer, M., Earnest, T.M., Merryman, C., Wise, K.S., Sun, L., Lynott, M.R., Hutchison, C.A., Smith, H.O., Lapek, J.D., Gonzalez, D.J., et al. (2019). Essential metabolism for a minimal cell. eLife *8*, e36842.

Capra, E.J., and Laub, M.T. (2012). Evolution of two-component signal transduction systems. Annu. Rev. Microbiol. *66*, 325–347.

Caspi, Y., and Dekker, C. (2014). Divided we stand: splitting synthetic cells for their proliferation. Syst. Synth. Biol. *8*, 249–269.

Chalfoun, J., Majurski, M., Peskin, A., Breen, C., Bajcsy, P., and Brady, M. (2015). Empirical gradient threshold technique for automated segmentation across image modalities and cell lines. J. Microsc. *260*, 86–99.

Chen, I.A. (2009). Cell division: breaking up is easy to do. Curr. Biol. *19*, R327–R328.

Chen, Y., Zhang, S., Young, E.M., Jones, T.S., Densmore, D., and Voigt, C.A. (2020). Genetic circuit design automation for yeast. Nat. Microbiol. *5*, 1349–1360.

Dienes, L., and Bullivant, S. (1968). Morphology and reproductive processes of the L forms of bacteria. II. Comparative study of L forms and Mycoplasma with the electron microscope. J. Bacteriol. *95*, 672–687.

Duman, R., Ishikawa, S., Celik, I., Strahl, H., Ogasawara, N., Troc, P., Löwe, J., and Hamoen, L.W. (2013). Structural and genetic analyses reveal the protein SepF as a new membrane anchor for the Z ring. Proc. Natl. Acad. Sci. USA *110*, E4601–E4610.

Dybvig, K., Zuhua, C., Lao, P., Jordan, D.S., French, C.T., Tu, A.H., and Loraine, A.E. (2008). Genome of *Mycoplasma arthritidis*. Infect. Immun. *76*, 4000–4008.

Eraso, J.M., Markillie, L.M., Mitchell, H.D., Taylor, R.C., Orr, G., and Margolin, W. (2014). The highly conserved MraZ protein is a transcriptional regulator in *Escherichia coli*. J. Bacteriol. *196*, 2053–2066.

Ernst, R., Ejsing, C.S., and Antonny, B. (2016). Homeoviscous adaptation and the regulation of membrane lipids. J. Mol. Biol. *428* (24 Pt A), 4776–4791.

Errington, J. (2017). Cell wall-deficient, L-form bacteria in the 21st century: a personal perspective. Biochem. Soc. Trans. *45*, 287–295.

Fredens, J., Wang, K., de la Torre, D., Funke, L.F.H., Robertson, W.E., Christova, Y., Chia, T., Schmied, W.H., Dunkelmann, D.L., Beránek, V., et al. (2019). Total synthesis of *Escherichia coli* with a recoded genome. Nature *569*, 514–518.

Gibson, D.G., Glass, J.I., Lartigue, C., Noskov, V.N., Chuang, R.Y., Algire, M.A., Benders, G.A., Montague, M.G., Ma, L., Moodie, M.M., et al. (2010). Creation of a bacterial cell controlled by a chemically synthesized genome. Science *329*, 52–56.

Gietz, R.D., and Schiestl, R.H. (2007). Large-scale high-efficiency yeast transformation using the LiAc/SS carrier DNA/PEG method. Nat. Protoc. *2*, 38–41.

Hamoen, L.W., Meile, J.C., de Jong, W., Noirot, P., and Errington, J. (2006). SepF, a novel FtsZ-interacting protein required for a late step in cell division. Mol. Microbiol. *59*, 989–999.

Housman, M., Milam, S.L., Moore, D.A., Osawa, M., and Erickson, H.P. (2016). FtsZ protofilament curvature is the opposite of tubulin rings. Biochemistry *55*, 4085–4091.

Hrabak, E.M., and Willis, D.K. (1992). The *lemA* gene required for pathogenicity of *Pseudomonas syringae* pv. *syringae* on bean is a member of a family of two-component regulators. J. Bacteriol. *174*, 3011–3020.

Hürtgen, D., Härtel, T., Murray, S.M., Sourjik, V., and Schwille, P. (2019). Functional modules of minimal cell division for synthetic biology. Adv. Biosyst. *3*, e1800315.

Hussain, S., Wivagg, C.N., Szwedziak, P., Wong, F., Schaefer, K., Izoré, T., Renner, L.D., Holmes, M.J., Sun, Y., Bisson-Filho, A.W., et al. (2018). MreB filaments align along greatest principal membrane curvature to orient cell wall synthesis. eLife *7*, e32471.

Hutchison, C.A., 3rd, Chuang, R.Y., Noskov, V.N., Assad-Garcia, N., Deerinck, T.J., Ellisman, M.H., Gill, J., Kannan, K., Karas, B.J., Ma, L., et al. (2016). Design and synthesis of a minimal bacterial genome. Science *351*, aad6253.

Kang, K.S., and Casida, L.E., Jr. (1967). Large bodies of Mycoplasma and L-form organisms. J. Bacteriol. *93*, 1137–1142.

Kannan, K., Tsvetanova, B., Chuang, R.Y., Noskov, V.N., Assad-Garcia, N., Ma, L., Hutchison Iii, C.A., Smith, H.O., Glass, J.I., Merryman, C., et al. (2016). One step engineering of the small-subunit ribosomal RNA using CRISPR/Cas9. Sci. Rep. *6*, 30714.

Karas, B.J., Jablanovic, J., Sun, L., Ma, L., Goldgof, G.M., Stam, J., Ramon, A., Manary, M.J., Winzeler, E.A., Venter, J.C., et al. (2013). Direct transfer of whole genomes from bacteria to yeast. Nat. Methods *10*, 410–412.

Karas, B.J., Wise, K.S., Sun, L., Venter, J.C., Glass, J.I., Hutchison, C.A., 3rd, Smith, H.O., and Suzuki, Y. (2014). Rescue of mutant fitness defects using in vitro reconstituted designer transposons in *Mycoplasma mycoides*. Front. Microbiol. *5*, 369.

Kolnik, M., Tsimring, L.S., and Hasty, J. (2012). Vacuum-assisted cell loading enables shear-free mammalian microfluidic culture. Lab Chip *12*, 4732–4737.

Kostylev, M., Otwell, A.E., Richardson, R.E., and Suzuki, Y. (2015). Cloning Should Be Simple: Escherichia coli DH5α-Mediated Assembly of Multiple DNA Fragments with Short End Homologies. PLoS ONE *10*, e0137466.

Krupka, M., and Margolin, W. (2018). Unite to divide: Oligomerization of tubulin and actin homologs regulates initiation of bacterial cell division. F1000Res. *7*, 235.

Lartigue, C., Vashee, S., Algire, M.A., Chuang, R.Y., Benders, G.A., Ma, L., Noskov, V.N., Denisova, E.A., Gibson, D.G., Assad-Garcia, N., et al. (2009). Creating bacterial strains from genomes that have been cloned and engineered in yeast. Science *325*, 1693–1696.

Leaver, M., Domínguez-Cuevas, P., Coxhead, J.M., Daniel, R.A., and Errington, J. (2009). Life without a wall or division machine in *Bacillus subtilis*. Nature *457*, 849–853.

Lipowsky, R. (2013). Spontaneous tubulation of membranes and vesicles reveals membrane tension generated by spontaneous curvature. Faraday Discuss. *161*, 305–331, discussion 419–459.

Loose, M., and Mitchison, T.J. (2014). The bacterial cell division proteins FtsA and FtsZ self-organize into dynamic cytoskeletal patterns. Nat. Cell Biol. *16*, 38–46.

Mali, P., Yang, L., Esvelt, K.M., Aach, J., Guell, M., DiCarlo, J.E., Norville, J.E., and Church, G.M. (2013). RNA-guided human genome engineering via Cas9. Science *339*, 823–826.

Margolin, W. (2020). Bacterial division: Journey to the center of the cell. Curr. Biol. *30*, R114–R116.

Mercier, R., Kawai, Y., and Errington, J. (2013). Excess membrane synthesis drives a primitive mode of cell proliferation. Cell *152*, 997–1007.

Nielsen, A.A., Der, B.S., Shin, J., Vaidyanathan, P., Paralanov, V., Strychalski, E.A., Ross, D., Densmore, D., and Voigt, C.A. (2016). Genetic circuit design automation. Science *352*, aac7341.

Noireaux, V., and Liu, A.P. (2020). The new age of cell-free biology. Annu. Rev. Biomed. Eng. *22*, 51–77.

Noskov, V.N., Ma, L., Chen, S., and Chuang, R.Y. (2015). Recombinase-mediated cassette exchange (RMCE) system for functional genomics studies in *Mycoplasma mycoides*. Biol. Proced. Online *17*, 6.

Osawa, M., and Erickson, H.P. (2018). Turgor pressure and possible constriction mechanisms in bacterial division. Front. Microbiol. *9*, 111.

Ostrov, N., Landon, M., Guell, M., Kuznetsov, G., Teramoto, J., Cervantes, N., Zhou, M., Singh, K., Napolitano, M.G., Moosburner, M., et al. (2016). Design, synthesis, and testing toward a 57-codon genome. Science *353*, 819–822.

Randall, G.C., and Doyle, P.S. (2005). Permeation-driven flow in poly(dimethylsiloxane) microfluidic devices. Proc. Natl. Acad. Sci. USA *102*, 10813–10818.

Razin, S., Cosenza, B.J., and Tourtellotte, M.E. (1967). Filamentous growth of mycoplasma. Ann. N Y Acad. Sci. *143*, 66–72.

Ruiz-Herrero, T., Fai, T.G., and Mahadevan, L. (2019). Dynamics of growth and form in prebiotic vesicles. Phys. Rev. Lett. *123*, 038102.

Sekar, K., Rusconi, R., Sauls, J.T., Fuhrer, T., Noor, E., Nguyen, J., Fernandez, V.I., Buffing, M.F., Berney, M., Jun, S., et al. (2018). Synthesis and degradation

of FtsZ quantitatively predict the first cell division in starved bacteria. Mol. Syst. Biol. *14*, e8623.

Seto, S., and Miyata, M. (1998). Cell reproduction and morphological changes in *Mycoplasma capricolum*. J. Bacteriol. *180*, 256–264.

Seto, S., and Miyata, M. (1999). Partitioning, movement, and positioning of nucleoids in *Mycoplasma capricolum*. J. Bacteriol. *181*, 6073–6080.

Shaner, N.C., Campbell, R.E., Steinbach, P.A., Giepmans, B.N., Palmer, A.E., and Tsien, R.Y. (2004). Improved monomeric red, orange and yellow fluorescent proteins derived from Discosoma sp. red fluorescent protein. Nat. Biotechnol. *22*, 1567–1572.

Si, F., Le Treut, G., Sauls, J.T., Vadia, S., Levin, P.A., and Jun, S. (2019). Mechanistic origin of cell-size control and homeostasis in bacteria. Curr. Biol. *29*, 1760–1770.

Singh, J.K., Makde, R.D., Kumar, V., and Panda, D. (2008). SepF increases the assembly and bundling of FtsZ polymers and stabilizes FtsZ protofilaments by binding along its length. J. Biol. Chem. *283*, 31116–31124.

Szwedziak, P., Wang, Q., Freund, S.M., and Löwe, J. (2012). FtsA forms actin-like protofilaments. EMBO J. *31*, 2249–2260.

Tsarmpopoulos, I., Gourgues, G., Blanchard, A., Vashee, S., Jores, J., Lartigue, C., and Sirand-Pugnet, P. (2016). In-yeast engineering of a bacterial genome using CRISPR/Cas9. ACS Synth. Biol. *5*, 104–109.

Vedyaykin, A., Ponomareva, E., Khodorkovskii, M., Borchsenius, S., and Vishnyakov, I. (2019). Mechanisms of bacterial cell division. Microbiology *88*, 245–260.

Wang, P., Robert, L., Pelletier, J., Dang, W.L., Taddei, F., Wright, A., and Jun, S. (2010). Robust growth of *Escherichia coli*. Curr. Biol. *20*, 1099–1103.

Wu, L.J., Lee, S., Park, S., Eland, L.E., Wipat, A., Holden, S., and Errington, J. (2020). Geometric principles underlying the proliferation of a model cell system. Nat. Commun. *11*, 4149.

Yang, J., Suzuki, M., and McCarty, D.R. (2016). Essential role of conserved DUF177A protein in plastid 23S rRNA accumulation and plant embryogenesis. J. Exp. Bot. *67*, 5447–5460.

Zhang, Y.M., and Rock, C.O. (2008). Membrane lipid homeostasis in bacteria. Nat. Rev. Microbiol. *6*, 222–233.

Please cite this article in press as: Pelletier et al., Genetic requirements for cell division in a genomically minimal cell, Cell (2021), https://doi.org/10.1016/j.cell.2021.03.008

STAR★METHODS

KEY RESOURCES TABLE

REAGENT or RESOURCE	SOURCE	IDENTIFIER
Bacterial and virus strains		
JCVI-syn1.0	Gibson et al., 2010	GenBank: CP002027
JCVI-syn3.0	Hutchison et al., 2016	GenBank: CP014940.1
RGD1-8	Hutchison et al., 2016	N/A
JCVI-syn3A	This study; Breuer et al., 2019	GenBank: CP016816.2
JCVI-syn3.0+1	This study	N/A
JCVI-syn3.0+126	This study	N/A
JCVI-syn3A ΔCluster1	This study	N/A
JCVI-syn1.0+mCherry	This study	N/A
JCVI-syn3.0+mCherry	This study	N/A
RGD6+mCherry	This study	N/A
JCVI-syn3.0+12345678	This study	N/A
JCVI-syn3.0+124678	This study	N/A
JCVI-syn3.0+1267	This study	N/A
JCVI-syn3.0+1	This study	N/A
JCVI-syn3.0+2	This study	N/A
JCVI-syn3.0+6	This study	N/A
JCVI-syn3.0+267	This study	N/A
JCVI-syn3.0+167	This study	N/A
JCVI-syn3.0+127	This study	N/A
JCVI-syn3.0+126 Δ602	This study	N/A
JCVI-syn3.0+126 Δ604	This study	N/A
JCVI-syn3.0+126 Δ605	This study	N/A
JCVI-syn3.0+126 Δ602 Δ604	This study	N/A
JCVI-syn3.0+126 Δ604 Δ605	This study	N/A
JCVI-syn3.0+126 Δ602 Δ605	This study	N/A
JCVI-syn3.0+126 Δ521 Δ522	This study	N/A
JCVI-syn3.0+126 Δ520 Δ522	This study	N/A
JCVI-syn3.0+126 Δ520	This study	N/A
JCVI-syn3.0+126 Δ521	This study	N/A
JCVI-syn3.0+126 Δ522	This study	N/A
JCVI-syn3.0+126 Δ520 Δ521	This study	N/A
JCVI-syn3A ΔCluster2	This study	N/A
JCVI-syn3A ΔCluster3	This study	N/A
JCVI-syn3A ΔCluster4	This study	N/A
JCVI-syn3A ΔCluster5	This study	N/A
JCVI-syn3A ΔCluster6	This study	N/A
JCVI-syn3A ΔCluster7	This study	N/A
JCVI-syn3A ΔCluster8	This study	N/A
DH5alpha competent *E. coli* (High efficiency)	New England Biolabs	Cat#C2987H
ElectroMAX Stbl4 competent *E. coli*	Thermo Fisher Scientific	Cat#11635018
Chemicals, peptides, and recombinant proteins		
Tetracycline	Sigma-Aldrich	Cat#87128
Puromycin	Sigma-Aldrich	Cat#P8833

(*Continued on next page*)

Please cite this article in press as: Pelletier et al., Genetic requirements for cell division in a genomically minimal cell, Cell (2021), https://doi.org/10.1016/j.cell.2021.03.008

Continued

REAGENT or RESOURCE	SOURCE	IDENTIFIER
Ampicillin	Sigma-Aldrich	Cat#A9393
Chloramphenicol	Sigma-Aldrich	Cat#C0378
Sodium cacodylate	Sigma-Aldrich	Cat#C0250
Osmium tetroxide	Sigma-Aldrich	Cat#201030
Polydimethylsiloxane	Sylgard	Cat#184
Poly-L-lysine-g-polyethylene glycol	SuSoS	PLL(20)-g[3.5]-PEG(5)
Phenol red	Sigma-Aldrich	Cat#P5530
Hoechst 33258	Thermo Fisher Scientific	Cat#H1398
SP-DiOC18(3)	Thermo Fisher Scientific	Cat#D7778
Polyethylene glycol 6000	Sigma-Aldrich	Cat#528877
Tn5 transposase	ABP Biosciences	Cat#TN501
Zymolyase-20T solution	USBiological	Cat#37340-57-1
Turbo DNase	Thermo Fisher Scientific	Cat#AM2239
Acid-Phenol:Chloroform	Thermo Fisher Scientific	Cat#AM9720
Critical commercial assays		
PrimeSTAR Max DNA Polymerase	Takara	Cat#R045B
DNA Clean & Concentrator Kit	Zymo Research	Cat#D4013
Taq 2X Master Mix	New England Biolabs	Cat#M0270L
QIAprep Spin Miniprep Kit	QIAGEN	Cat#27106
QIAGEN Multiplex PCR Kit	QIAGEN	Cat#206145
Q5 High-Fidelity 2X Master Mix	New England Biolabs	Cat#M0492L
T7 RiboMAX Express Large Scale RNA Production System	Promega Corporation	Cat#P1320
Qubit RNA HS Assay Kit	Thermo Fisher Scientific	Cat#Q32852
Deposited data		
JCVI-syn1.0	Gibson et al., 2010	GenBank: CP002027
JCVI-syn3.0	Hutchison et al., 2016	GenBank: CP014940.1
JCVI-syn3A	Breuer et al., 2019	GenBank: CP016816.2
Experimental models: organisms/strains		
S. cerevisiae VL6_48N_cas9	Daniel Gibson (Codex DNA, Inc.)	N/A
Oligonucleotides		
For PCR primers, see Table S1	Integrated DNA Technologies	N/A
Recombinant DNA		
Pmod2-loxpurolox-sp-cre	Hutchison et al., 2016	GenBank: MN982903.1
pTF20	Dybvig et al., 2008	N/A
pLS-Tn5-Puro	Karas et al., 2014	N/A
Pmod2-MCS	Epicenter	Cat#TNP10622
PCC1BAC_trp	Billyana Tsvetanova (SGI-DNA, Inc.)	GenBank: MN982904
PRS316 bearing *ura3* marker	ATCC	Cat#77145
Plasmids developed in this study in Table S1	This study	N/A
Software and algorithms		
Empirical gradient threshold (EGT)	Chalfoun et al., 2015; Mendeley Data: https://doi.org/10.17632/rwg6sdz4rf.1	https://isg.nist.gov/deepzoomweb/resources/csmet/pages/EGT_segmentation/EGT_segmentation.html
MATLAB	MathWorks	https://www.mathworks.com/products/matlab.html
WordPerfect macros	Hutchison et al., 2016	http://www.wordperfect.com/en/
QIAGEN CLC Genomics Workbench	QIAGEN	https://digitalinsights.qiagen.com/products-overview/discovery-insights-portfolio/analysis-and-visualization/qiagen-clc-genomics-workbench/

Please cite this article in press as: Pelletier et al., Genetic requirements for cell division in a genomically minimal cell, Cell (2021), https://doi.org/10.1016/j.cell.2021.03.008

RESOURCE AVAILABILITY

Lead contact

Further information and requests for resources and reagents should be directed to and will be fulfilled by the Lead Contact, Elizabeth A. Strychalski (elizabeth.strychalski@nist.gov).

Materials availability

Bacterial strains will be made available to qualified researchers by the JCVI and Codex DNA, Inc. under a material transfer agreement. Note that United States scientists must obtain a United States Veterinary Permit for Importation and Transportation of Controlled Materials and Organisms and Vectors from the U.S. Department of Agriculture Animal and Plant Health Inspection Service. The organisms require Biosafety Level 2 containment.

Data and code availability

Source data and analysis code for Figures 1D, 4D, and 5E, as well as additional videos showing cell propagation in microfluidic chemostats, are available on Mendeley Data: https://doi.org/10.17632/rwg6sdz4rf.1. GenBank: CP016816.2 includes the genome sequence of JCVI-syn3A with the most updated gene annotations.

EXPERIMENTAL MODEL AND SUBJECT DETAILS

Bacterial strains and growth media

The principal mycoplasmal strains used in this study are JCVI-syn1.0 (GenBank: CP002027), JCVI-syn3.0 (GenBank: CP014940.1), and JCVI-syn3A (GenBank: CP016816.2). Chromosomes of all strains and their derivatives carry a yeast *CEN/ARS* and a *his3* marker for centromeric propagation of the genome in yeast, as well as a *tetM* resistance marker for selection after genome transplantation into a mycoplasma recipient. Mycoplasmal strains were propagated in SP4 medium containing fetal bovine serum (hereafter SP4), as previously described (Hutchison et al., 2016).

METHOD DETAILS

Microscopy of bulk cultures

Mycoplasma transplants were grown in static, planktonic culture at 37°C in SP4 liquid medium without tetracycline. To observe cell morphologies in culture with minimal manipulation, wet mounts were prepared from logarithmic phase cultures after 3 days of growth, by depositing 3 μL of settled cells, which had been carefully removed by micropipette tip from round-bottom culture tubes, onto an untreated glass slide and applying an 18 × 18 mm coverslip. Optical microscopy was performed using a Zeiss Axio Imager 1 microscope with a Zeiss plan-apochromatic 63x oil 1.4 objective, differential interference contrast (DIC) optics and X-Cite 120PC Q mercury arc lamp. A 43HE filter with excitation BP 550/25 (HE) and emission BP 605/70 (HE) was used to detect fluorescence in constructs containing mCherry.

Scanning electron imaging

Cells grown in SP4 medium were centrifuged at room temperature for 4 min at 2000 g to produce a loose pellet. 1 mL of fixative solution consisting of 2.5 % (w/v) glutaraldehyde, 100 mmol/L sodium cacodylate, 2 mmol/L calcium chloride, and 2 % (w/v) sucrose was added cold and replaced 950 μL of growth medium. Samples were subsequently stored at 4°C. Imaging substrates were glass coverslips coated with indium tin oxide and treated with polyethylenimine or poly-D-lysine. (10 to 20) μL of solution containing cells were placed on top of the coverslips for 2 min and subsequently washed five times for 2 min each on ice using 0.1 mol/L cacodylate buffer with 2 mmol/L calcium chloride and 2 % (w/v) sucrose. Cells were fixed further on ice in 2 % (w/v) osmium tetroxide with 2 % (w/v) sucrose in 0.1 mol/L cacodylate for 30 min, followed by rinsing with double distilled water and dehydration in an ethanol series of (20, 50, 70, and 100) % (v/v) for 2 min each on ice. Substrates with immobilized cells were then dried through the critical point with carbon dioxide and sputter-coated with a thin layer of Au/Pd. Images were collected with a Zeiss Merlin Fe-SEM at 2.5 keV, 83 pA probe current, and 2.9 mm working distance using zero tilt and the secondary electron detector.

Microfluidic platform fabrication

We fabricated microfluidic chemostats to culture and image the growth of genomically minimized mycoplasmas in a shear-free, biochemically controlled environment (Figure S1). Shallow growth chambers confined cells to facilitate imaging, while deeper microfluidic channels loaded cells, perfused fresh growth media, and introduced fluorescent labels to determine the spatial distribution of cytoplasmic protein, nucleoids, membrane, and extracellular growth medium. The concept of the device is similar to previous microfluidic chemostats (Wang et al., 2010), with the exception cells in our chambers were free to diffuse.

Soft lithographic processing allowed facile fabrication and characterization of devices compatible with cell growth and optical imaging. A negative master was fabricated on a silicon wafer, using reactive ion etching to define 3.1 μm deep chambers arrayed along

Please cite this article in press as: Pelletier et al., Genetic requirements for cell division in a genomically minimal cell, Cell (2021), https://doi.org/10.1016/j.cell.2021.03.008

a 100 μm wide by 22 μm deep channel defined by SU-8 photoresist (MicroChem). After treating with a silane release layer, a positive mold of the device was created in polydimethylsiloxane (PDMS, Sylgard 184) and bonded irreversibly to a #1.5 borosilicate coverslip after treatment with an oxygen plasma. Correcting for known 1.4 % shrinkage after curing at 80°C, chamber and channel depths decrease to 3.0 μm and 21 μm, respectively. The lateral dimensions of the chambers ensured rapid diffusive exchange with the deeper channel and are visible in Figures 1, 3, 4, and S1, and Videos S1, S2, S3, and S4. Devices were filled with fluid immediately, to take advantage of the small liquid contact angle after plasma treatment.

Microfluidic cell culture and imaging

Cells were imaged using an inverted microscope outfitted with an incubator and heated stage, set to 37.0°C, vibration isolation workstation, 100x magnification objective (Zeiss, alpha Plan-Apochromat, 1.46 numerical aperture, oil immersion), suitable LED excitation sources and emission filter cubes, and a water-cooled sCMOS camera (Hamamatsu Orca Flash 4.0 v2). Cells were grown in SP4 medium, but with the pH indicator dye phenol red omitted to reduce background fluorescence. Image acquisition was automated using Zeiss Zen software and automated focus correction, for multichannel, timelapse imaging of overnight growth experiments over ≈(10 to 16) h, with images taken every ≈(10 to 30) min, as well as endpoint staining with fluorescent dyes. As appropriate to each strain, cells were imaged overnight in transilluminated brightfield and fluorescence, to image the cytoplasm of cells expressing mCherry. Endpoint fluorescence labels included 10 μg/mL Hoechst 33258 (Life Technologies) to visualize DNA, 84 μg/mL SP-DiOC18(3) (Life Technologies) to visualize membranes, and FITC-Dextran (10 kDa molecular weight) to image the negative space around cells. Cells were incubated with the fluorescent dyes for ≈(5 to 100) min in SP4 medium or in PBS or Tris sucrose buffer (10 mmol/L Tris pH 6.5 and 0.5 mol/L sucrose) to reduce background fluorescence. Strains expressing mCherry exhibited qualitatively similar morphological features as strains without mCherry, so mCherry strains were useful to investigate the composition of different morphotypes.

Typically, device surfaces were functionalized with 0.1 mg/mL poly-L-lysine-g-polyethylene glycol (SuSoS) in 10 mmol/L HEPES pH 7.4 soon after bonding, to prevent cell adhesion. After incubating for 40 min with PLL-g-PEG, devices were flushed with sterile water, followed by SP4 growth medium and cells in the same growth medium. For microfluidic cell culture, SP4 medium was prepared without phenol red, to reduce background signal during fluorescence imaging. Cells entered the chambers diffusively at room temperature for ≈(5 to 60) min, depending on the typical cell size, cell concentration in the loading channel, and the desired number of cells per chamber. Devices mounted on a microscope for cell growth and imaging were infused with fresh growth medium at 200 μL/hr using a syringe pump.

The small submicrometer cells diffused freely in the chambers but tended to congregate opposite the chamber entrance, likely due to a small net fluid flow into the bulk device material (Kolnik et al., 2012; Randall and Doyle, 2005). Thus, in contrast to related mother machine devices (Wang et al., 2010), the number of cells per chamber increased over time.

Genome synthesis and assembly

The synthesis and assembly of minimized genomes has been described previously (Hutchison et al., 2016). Briefly, overlapping oligonucleotides of < 80 bases were designed using WordPerfect macros (Hutchison et al., 2016). Streamlined oligonucleotide design software was also embedded in the Archetype® software available commercially through Codex DNA, Inc. Then, oligonucleotides were purchased (Integrated DNA Technologies), pooled, assembled into 1.4 kilobase fragments, error corrected, and amplified. These fragments were subsequently assembled into 7 kilobase cassettes using Gibson Assembly and cloned in *E. coli*. These cassettes were further assembled into genome segments and whole genomes in *S. cerevisiae*.

Construction of genomes by combining segments

The final assembly of whole genomes by combining chromosome segments has been described previously (Hutchison et al., 2016). The complete genome sequences of JCVI-syn1.0 and the minimal JCVI-syn3.0, comprised of a combination of each minimal segment 1 through 8, are available through GenBank (Table S1). Additional constructs were made (Hutchison et al., 2016) by placing each of the eight fully minimized segments into a genome containing the seven other unminimized segments of the JCVI-syn1.0 genome. One resulting strain contains a minimal segment 6 in an otherwise unminimized genome (RGD6) and is further characterized here. Another construct, JCVI-syn3A, comprises the minimal JCVI-syn3.0 genome whose segment 6 is replaced with an alternate version that includes 19 additional genes. The complete genome sequence of this construct is available through GenBank (Table S1) and represents the most recent and accurate annotation of genes.

Gene additions to JCVI-syn3.0

JCVI-syn3.0 subclone 13-2, referred to simply as JCVI-syn3.0 in this study, contains two hetero-specific *loxP* sites that comprise a landing pad between genes *601* and *606*, which are adjacent in the fully minimized JCVI-syn3.0 genome (Hutchison et al., 2016; Noskov et al., 2015). Plasmid Pmod2-loxpurolox-sp-cre (annotated sequence in GenBank: MN982903.1) includes the puromycin resistance marker flanked by two hetero-specific *loxP* sites and serves as a vector to transfer gene cassettes into JCVI-syn3.0 using Cre recombinase/*loxP*-mediated recombination. After transformation into recipient JCVI-syn3.0 cells, the *loxP*-flanked cassette in the plasmid inserts into the genome, replacing the *loxP*-flanked region in the genome.

Please cite this article in press as: Pelletier et al., Genetic requirements for cell division in a genomically minimal cell, Cell (2021), https://doi.org/10.1016/j.cell.2021.03.008

Transformation of JCVI-syn3.0 using plasmids

Cells were transformed as described previously (Hutchison et al., 2016). Briefly, JCVI-syn3.0 cells were grown in 4 mL of SP4 growth medium to reach pH 6.5 to pH 7.0. The culture was centrifuged for 15 min at 4700 rpm and 10°C in a 50 mL centrifuge tube. The pellet was resuspended in 3 mL of Sucrose/Tris (S/T) Buffer, composed of 0.5 mol/L sucrose and 10 mmol/L Tris at pH 6.5. The resuspended cells were centrifuged for 15 min at 5369 g and 10°C. The supernatant was discarded, and the pellet resuspended in 250 μL of 0.1 mol/L $CaCl_2$ and incubated for 30 min on ice. Then, 200 ng of plasmid was added to the cells, and the centrifuge tube was mixed gently. 2 mL of 70 % (w/v) polyethylene glycol (PEG) 6000 (Sigma), dissolved in S/T Buffer, was added to the centrifuge tube, and mixed well using a serological pipette. After a 2 min incubation at room temperature, 20 mL S/T Buffer without PEG was added immediately and mixed well. The tube was centrifuged for 15 min at 10,000 g and 8°C. The supernatant was discarded, and the tube inverted with the cap removed on tissue paper to drain residual PEG. The cells were subsequently resuspended in 1 mL of SP4 growth medium prewarmed to 37°C. These cells were incubated for 2 h at 37°C, followed by plating on SP4 agar containing 3 μg/mL of puromycin (Sigma). Colonies appeared after 3 to 4 days at 37°C.

Construction of plasmids

Construction of plasmid Pmod2-loxpurolox-sp-cre_520-522 (cluster 1)

The plasmid Pmod2-loxpurolox-sp-cre_*520-522* was constructed by inserting the genes *520-522* adjacent to the puromycin resistance marker in plasmid Pmod2-loxpurolox-sp-cre via assembly as previously described (Kostylev et al., 2015). The genome cassette spanning genes *520-522* was amplified with primers M_520_F and M_520_R, PrimeSTAR Max Premix (Takara), and using JCVI-syn1.0 genomic DNA as the template. PCR conditions were: 98°C for 2 min; 30 cycles of 98°C for 10 s, 55°C for 10 s, and 72°C for 1 min; and, 72°C for 2 min. The linear vector Pmod2-loxpurolox-sp-cre was amplified using primers M_v_F and M_v_R, PrimeSTAR Max Premix, and using the plasmid Pmod2-loxpurolox-sp-cre as the template. PCR conditions were: 98°C for 2 min; 30 cycles of 98°C for 10 s, 58°C for 10 s, and 72°C for 1 min; and, 72°C for 2 min. The PCR product for the linear vector was mixed with 1 μL of DpnI and incubated at 37°C for 1 h to digest the plasmid template. The PCR amplicon was purified using a DNA Clean & Concentrator Kit (Zymo Research). Purified DNA fragment *520-522* and linear vector were introduced by transformation into competent cell DH5alpha C2987H (New England Biolabs). 1 mL of SOC (Thermo Fisher Scientific) was added to the transformation mix, and, after incubation at 37°C for 1 h, cells were plated on AmpR LB agar plates and incubated at 37°C overnight. Colony PCR was used to screen surviving transformants for the presence of the *520-522* insert using primers spanning the insert junctions and amplification with Taq 2X Master Mix PCR Kit (New England Biolabs), as described by the supplier. The PCR conditions were: 94°C for 3 min; 30 cycles of 94°C for 15 s, 55°C for 20 s, and 68°C for 30 s; and, followed by 68°C for 1 min. The expected DNA sizes are listed in Table S1. Positive clones with the predicted 330 bp DNA band indicating the insertion of genes *520-522* were identified. Plasmids from positive clones were extracted using a QIAGEN Mini-Prep Kit by the manual. Sanger sequencing of plasmids confirmed the absence of mutations. Primers for PCR amplification, junction colony PCR, and sequencing are listed in Table S1.

Construction of plasmid Pmod2-loxpurolox-sp-cre_602-605 (cluster 6)

The plasmid Pmod2-loxpurolox-sp-cre_*602-605* was constructed by inserting the genes *602-605* adjacent to the puromycin resistance marker in Pmod2-loxpurolox-sp-cre via Gibson Assembly. The genes *602-605* were amplified using primers 0602_fwd and 0605_rev, PrimeSTAR Max Premix, and JCVI-syn1.0 genome as the template. The linear vector Pmod2-loxpurolox-sp-cre was PCR amplified using primers vec_fwd and vec_rev, PrimeSTAR Max Premix, and the plasmid Pmod2-loxpurolox-sp-cre as the template. The PCR conditions were: 98°C for 2 min; 30 cycles of 98°C for 10 s, 55°C for 20 s, and 72°C for 40 s; and, followed by 72°C for 5 min. Zymo DNA Clean & Concentrator Kit purified DNA fragment *602-605* and gel purified linear vector were assembled via Gibson Assembly. The assembly mix was transformed using competent cell DH5alpha C2987H, grown at 37°C for 1 h and plated on an AmpR LB plate. The plate was incubated at 37°C overnight. Colony PCR was used to screen positive colonies with genes *602-605* insertion in vector using junction primers and QIAGEN Multiplex PCR Kit by the manual. The expected DNA sizes are listed in Table S1. Positive clones showing the 335 bp and 507 bp PCR products that confirmed genes *602-605* insertion were obtained. Plasmids from positive clones were extracted using a QIAGEN Mini-Prep Kit. Sanger sequencing of the plasmids confirmed the absence of mutations. Primers for PCR amplification, colony PCR, and sequencing are listed in Table S1.

Construction of plasmid Pmod2-loxpurolox-sp-cre_538+546-549+592-593+622-623 (clusters 3+4+5+8)

The plasmid Pmod2-loxpurolox-sp-cre_*538+546-549+592-593+622-623* was constructed by inserting the genes *538*, *546-549*, *592-593*, and *622-623* adjacent to the puromycin resistance marker in Pmod2-loxpurolox-sp-cre via Gibson Assembly. The region containing genes *538*, *546-549*, *592-593*, and *622-623* was amplified using primers 622 F 6.9K and 592R 7.5 K, PrimeSTAR Max Premix, and plasmid Pmod2-hisarscen-*527_538_546-549_592-593_622-623* as the template. The linear vector Pmod2-loxpurolox-sp-cre was PCR amplified using primers vec F 7.5 K and vec R 6.9K, PrimeSTAR Max Premix, and the plasmid Pmod2-loxpurolox-sp-cre as the template. The PCR conditions were: 98°C 3 min; 30 cycles of 98°C for 10 s, 55°C for 10 s, and 72°C for 1 min; and, followed by 72°C for 2 min. The PCR amplicon was purified using a Zymo DNA Clean & Concentrator Kit.

Purified DNA fragment *538_546-549_592-593_622-623* and linear vector were assembled via Gibson Assembly. The assembly mix was transformed using competent cell DH5alpha C2987H, grown at 37°C for 1 h, and plated on an AmpR LB plate. The plate was incubated at 37°C overnight. Colony PCR was used to screen positive colonies containing the gene *538_546-549_592-593_622-623* insertion in the vector, using QIAGEN Multiplex PCR Kit according to the manufacturer's protocol. The expected sizes of

Please cite this article in press as: Pelletier et al., Genetic requirements for cell division in a genomically minimal cell, Cell (2021), https://doi.org/10.1016/j.cell.2021.03.008

PCR products listed in Table S1 were obtained. Primers for PCR amplification, colony PCR, and sequencing are listed in Table S1. Sanger sequencing data confirmed that the inserted genes in the plasmid had no mutations.

Construction of plasmid Pmod2-loxpurolox-sp-cre_546-549+622-623 (clusters 4+8)

The plasmid Pmod2-loxpurolox-sp-cre_*546-549+622-623* was constructed by inserting the genes *546-549*, and *622-623* adjacent to the puromycin resistance marker in Pmod2-loxpurolox-sp-cre via Gibson Assembly. The genes *546-549* were amplified using Q5 master mix, with JCVI-syn1.0 genome as the template, as well as primers 546 F to 622 and 546 R to 622. The genes *622-623* were amplified using Q5 master mix, with JCVI-syn1.0 as the template, and primers 622 F 6.9K and 622 R to 546. The linear vector Pmod2-loxpurolox-sp-cre was amplified using the plasmid Pmod2-loxpurolox-sp-cre as the template, Q5 master mix, and primers vec F 546-622 and vec R 6.9K. The PCR conditions were: 98°C 3 min; 30 cycles of 98°C for 10 s, 58°C for 15 s, and 72°C for 2.5 min; and, followed by 72°C for 3 min.

DNA fragments *546-549*, *622-623* and linear vector were assembled via Gibson Assembly. The assembly mix was transformed using competent cell DH5alpha C2987H, grown at 37°C for 1 h and plated on an AmpR LB plate. The plate was incubated at 37°C overnight. Colony PCR was used to screen positive colonies with a gene *546-549_622-623* insertion in the vector using a QIAGEN Multiplex PCR Kit protocol. The expected DNA sizes were listed in Table S1. Primers for PCR amplification, colony PCR and sequencing are listed in Table S1. Sanger sequencing confirmed that the plasmid has no mutations.

Confirmation of sequences in transformants

To confirm that the genes *520-522* or *602-605* and the puromycin resistance marker were inserted into the JCVI-syn3.0 genome after transformation, a diagnostic PCR with PrimeSTAR Max Premix was performed to screen positive colonies with the complete JCVI-syn3.0 genome, the genes *520-522* or *602-605*, and the puromycin resistance marker using transformant junction primers. For the cluster *520-522*, primers 0520_L(486) and pgk_R(486) were used. The PCR conditions were: 98°C for 2 min; 30 cycles of 98°C for 10 s, 55°C for 20 s, and 72°C for 30 s; and, followed by 72°C for 2 min. For cluster *602-605,* primers seq_F1 and puro_R were used. The PCR conditions were: 98°C for 2 min; 30 cycles of 98°C for 5 s, 55°C for 10 s, and 72°C for 40 s; and, followed by 72°C for 5 min.

The genomic DNA of positive colonies was extracted, and regions *520-522* or *602-605* were amplified via PCR with primers seq_F1 and puro_R and the Zymo DNA Clean & Concentrator Kit purified PCR product was sequenced. The PCR conditions were: 98°C for 2 min; 30 cycles of 98°C for 5 s, 55°C for 10 s, and 72°C for 40 s; and, followed by 72°C for 5 min. Sequencing results confirmed that *520-522* or *602-605* was inserted into the JCVI-syn3.0 genome without mutation. Primers used are listed in Table S1.

Construction of mCherry plasmid

Pmod2-loxpurolox-sp-cre_sp_mCherry was constructed by inserting the spiralen promoter and *mCherry* gene adjacent to the puromycin resistance marker in Pmod2-loxpurolox-sp-cre via Gibson Assembly. The spiralen promoter and *mCherry* gene were amplified using Q5 master mix (New England Biolabs), with the plasmid pTF20mChloxp as the template, based on the plasmid pTF20 (gift from Kevin Dybvig) (Dybvig et al., 2008). The linear vector Pmod2-loxpurolox-sp-cre was amplified using Q5 master mix, with plasmid Pmod2-loxpurolox-sp-cre as the template. Primers are listed in Table S1. The expected PCR product sizes listed in Table S1 were confirmed.

Insertion of mCherry into genomes

Insertion of mCherry into the JCVI-syn1.0 and RGD6 genomes

The mCherry coding sequence was introduced at random chromosomal locations into JCVI-syn1.0 or RGD6 cells and selected using the puromycin resistance marker, as described previously (Karas et al., 2014). Briefly, the coding sequence of mCherry (Shaner et al., 2004) was introduced into the pLS-Tn5-Puro vector (Karas et al., 2014), and a linearized product was then amplified and combined with Tn5 transposase. The resulting transposome was transformed into cells and plated on selective agar medium. Single colonies were picked and grown in liquid culture without selection and screened for suitable mCherry expression using fluorescence microscopy. JCVI-syn1.0+mCherry and RGD6+mCherry clonal isolates with bright fluorescence signals and stable expression of mCherry over many generations were used in the studies reported here.

Insertion of mCherry into the JCVI-syn3.0 genome

Transformation of JCVI-syn3.0 using Pmod2-loxpurolox-sp-cre_sp_mCherry plasmid was performed as described above. After transforming JCVI-syn3.0 cells with the plasmid Pmod2-loxpurolox-sp-cre_sp_mCherry, diagnostic PCR measurements confirmed delivery of the mCherry and puromycin resistance genes to the genome of JCVI-syn3.0+mCherry. Primers are listed in Table S1.

Construction of JCVI-syn3.0+12345678

Pmod2loxploxcre-*538+546-549+592-593+622-623* was used to transform JCVI-syn3.0+1267 (Figure 5C) to obtain JCVI-syn3.0+12345678 (Figure 5C). Junction PCR and Sanger sequencing showed that genes *puro* and *538+546-549+592-593+622-623* were inserted in the landing pad of JCVI-syn3.0+1267. The presence of the complete JCVI-syn3.0 genome was confirmed by colony multiplex PCR. Genomic DNA was extracted from the strain JCVI-syn3.0+12345678 and used as the template for PCR amplification of each gene. PrimeSTAR Max Premix, primers 7.8k LJF(401) and 520-602jR(326), 520-602jF(326) and 7.8k ploAR, 7.5k LJF(190) and 7.5k2jR(517), and seq_F1 and puro_R, respectively, were used to amplify regions containing each gene. PCR products were purified using a Zymo DNA Clean & Concentrator Kit. Sanger sequencing of PCR products, using primers for 7.5k in Table S1, excluding 7.5 K LJ F(190), revealed a single point mutation (G to T) in the intergenic region 5′ of gene *546*.

Please cite this article in press as: Pelletier et al., Genetic requirements for cell division in a genomically minimal cell, Cell (2021), https://doi.org/10.1016/j.cell.2021.03.008

Construction of JCVI-syn3.0+124678

Pmod2loxploxcre-*546-549+622-623* was used to transform JCVI-syn3.0+1267 to obtain JCVI-syn3.0+124678 (Figure 5C). Junction PCR and Sanger sequencing showed that gene puro and *546-549+622-623* were inserted in the landing pad of JCVI-syn3.0+1267. These strains were confirmed to have the complete JCVI-syn3.0 genome by colony multiplex PCR.

Genomic DNA was extracted from strain JCVI-syn3.0+124678. PrimeSTAR Max Premix, as well as primers seq_F1 and puro_R, were used to amplify added genes using the genomic DNA of JCVI-syn3.0+124678 as the template. PCR products were purified using a Zymo DNA Clean & Concentrator Kit. Sanger sequencing, using sequencing primers in Table S1, confirmed the absence of any mutations.

Editing mycoplasmal chromosomes in yeast

To put back several gene clusters in the genome of JCVI-syn3.0 in different locations, we used CRISPR/Cas9 to edit the genome of the mycoplasma in yeast. Editing the genome as a yeast centromeric plasmid clone (YCp) is required to delete genes from any synthetic strain or to insert genes at sites other than the dual *loxP* landing pad. After editing the genome as a YCp, the edited genome is transplanted into an *M. capricolum* recipient strain to render a mycoplasmal transplant programmed solely by the new chromosome.

The *S. cerevisiae* yeast strain VL6_48N_cas9 was obtained from Dr. Daniel G. Gibson (Codex DNA, Inc.). VL6_48N_cas9 carries the *cas9* gene in a yeast chromosome, which constitutively expresses Cas9 as described previously (Kannan et al., 2016). Yeast strains were grown in the yeast media "BD Difco™ YPD Broth (Fisher Scientific) plus 60 mg of adenine per liter," "c7112, CM Glucose Broth, Dry, Adenine-60, without Histidine," "c0230, CM Glucose Agar, Dry, w/o Histidine, Tryptophan," or "c7221, CM Glucose media, Dry, w/o Histidine, Uracil, 2 % (w/v) agar added to make agar plate." These media were all obtained from Teknova, unless indicated otherwise.

Insertion of bacterial genomes into yeast

To insert bacterial genomes into yeast, fusion of JCVI-syn3.0 or JCVI-syn3A with yeast strain VL6_48N_cas9 was performed as described elsewhere (Karas et al., 2013). Briefly, yeast VL6_48N_cas9 was grown overnight in YPD growth medium supplemented with adenine at 120 mg/L until OD600 ≈(1.0 to 2.0). Cells were centrifuged, and the supernatant was discarded. Cells were then washed in water and 1 mol/L sorbitol, followed by resuspension and centrifugation. The supernatant was discarded, and the cell pellet was then resuspended in SPEM solution, consisting of 1 mol/L sorbitol, 10 mmol/L EDTA, 2.08 g/L $Na_2HPO4 \cdot 7H_2O$, 0.32 g/L $NaH_2PO4 \cdot 1H_2O$, 30 μL of β-mercaptoethanol (Sigma-Aldrich), and 40 μL of Zymolyase-20T solution (200 mg Zymolyase (USB), 1 mL of 1 mol/L Tris-HCl pH 7.5, 10 mL 50 % (v/v) glycerol, and 9 mL dH_2O). After a 40 min incubation, the resulting yeast spheroplasts were ready for fusion to bacteria.

A 5 mL culture of JCVI-syn3.0 or JCVI-syn3A was grown overnight to pH (6.7 to 7.0). Chloramphenicol was then added to a final concentration of 100 mg/L, and cells were incubated at 37°C for 1.5 h. Cells were subsequently centrifuged and resuspended in 50 μL of 0.5X resuspension buffer, where 1X resuspension buffer is composed of 0.5 mol/L sucrose, 10 mmol/L Tris HCl pH 7.5, 10 mmol/L $CaCl_2$, and 2.5 mmol/L $MgCl_2$, with pH adjusted to pH 7.5.

200 μL of yeast spheroplasts and 50 μL of chloramphenicol-treated JCVI-syn3.0 or JCVI-syn3A cells were mixed gently. 1 mL of 20 % (w/v) PEG 8000 (USB) solution, consisting of 20 % (w/v) PEG 8000, 10 mmol/L Tris-HCl pH 8.0, 10 mmol/L $CaCl_2$, and 2.5 mmol/L $MgCl_2$, with pH adjusted to pH 8.0, was added to the yeast and mycoplasma mixture. After gentle mixing and further incubation at room temperature for 20 min, cells were centrifuged at 1500 g for 7 min and the supernatant removed. The cell pellet was resuspended in 1 mL of SOS, composed of 1 mol/L sorbitol, 6 mmol/L $CaCl_2$, 2.5 g/L yeast extract, and 5 g/L Bacto Peptone, and incubated for 30 min at 30°C. The 1 mL cell suspension in SOS was mixed with top agar and plated on agar plates containing CM Glucose Broth, Dry, Adenine-60, without Histidine with 1 mol/L sorbitol. Yeast transformants appeared after (3 to 5) days.

Yeast assembly of plasmids

Yeast assembly of Pmod2-hisarscen-610_520-522_602-605 (clusters 1+6+7)

Adding single gene clusters to JCVI-syn3.0 did not rescue the pleomorphic phenotype of JCVI-syn3.0. We therefore added multiple gene clusters to JCVI-syn3.0 in an attempt to correct this phenotype. We assembled several gene clusters in yeast. The genes *610, 520-522, 602-605* were amplified using amplification primers listed in Table S1 and PrimeSTAR Max Premix, with JCVI-syn1.0 genome as the template. The vector Pmod2-hisarscen was amplified using PrimeSTAR Max Premix with plasmid Pmod2-hisarscen-cm as the template, as well as primers Y 610 vec F and Y vec R in Table S1. The PCR conditions were: 98°C for 2 min; 30 cycles of 98°C for (5 or 10) s, 55°C for 10 s, and 72°C for (40 or 60) s; and, followed by 72°C for 3 min. The plasmid Pmod2-hisarscen-cm was constructed by assembly of *his*, *ars*, *cen,* and *cm* genes with vector Pmod2-MCS (Epicenter) via Gibson Assembly. The primers used for construction of Pmod2-hisarscen-cm are listed in Table S1. (25 to 50) ng of Zymo DNA Clean & Concentrator Kit purified DNA fragment *610, 520-522, 602-605* and linear vector Pmod2-hisarscen, with 50 bp overlapping with adjacent fragments, were assembled in yeast strain VL6_48 using the lithium acetate PEG method (Gietz and Schiestl, 2007). Plasmid was isolated from yeast, then transformed and propagated in *E. coli* STbl4 (Life Technology). Plasmid was then extracted for Sanger sequencing, which subsequently confirmed the absence of mutations. PCR amplification primers, junction primers for diagnostic PCR, and sequencing primers are listed in Table S1.

Yeast assembly of Pmod2-hisarscen-527_538_546-549_592-593_622-623 (clusters 2+3+4+5+8)

The gene clusters *527, 538, 546-549, 592-593* and *622-623* were amplified and assembled in yeast as described in the previous section. Diagnostic PCR with junction primers gave products with the expected sizes indicated in Table S1, thereby confirming

the correct assembly of genes *527, 538, 546-549, 592-593, 622-623*. Propagation of the plasmid in *E. coli* STbl4, followed by Sanger sequencing, confirmed the absence of mutations. PCR amplification primers, junction primers for diagnostic PCR, and sequencing primers are listed in Table S1.

Guide RNA production and quantification

We used CRISPR/Cas9 methods to insert genes into the JCVI-syn3.0 genome residing in the yeast strain VL6_48N_cas9_ JCVI-syn3.0. Initially, we designed single guide RNA (sgRNA) targeting the gene(s) of interest in the JCVI-syn3.0 genome. A (119 to 120) bp dsDNA was then obtained via a PCR reaction containing the following: 1 μL of the guide RNA forward primer 7.8k_gRNA_F (10 μmol/L) or 7.5k_gRNA_F (10 μmol/L), which included the T7 promoter, 19-20 bp guide RNA target, and an overlap with 83 bp of sgRNA_Template (Mali et al., 2013), 1 μL of reverse primer gRNA_R (10 μmol/L), 10 ng of 83 bp sgRNA template, and Q5 master mix or 2X PrimeSTAR Max Premix (Takara) in a 20 μL PCR reaction. The PCR conditions were: 2 min at 98°C; 30 cycles of 98°C for 10 s, 55°C for 10 s, and 72°C for 10 s; and, followed by 72°C for 5 min. We then purified the PCR amplicons using a Zymo DNA Clean & Concentrator Kit. We used 8 μL of the PCR amplicons as template in a 20 μL transcription reaction with the T7 RiboMAX Express Large Scale RNA Production System according to the manufacturer's instructions. Briefly, we combined 10 μL of RiboMAX Express T7 2X Buffer, 158 ng of the previously generated PCR amplicon (in 8 μL H_2O), and 2 μL Enzyme Mix T7 Express. The transcription reaction was incubated at 37 °C for 4 hr or overnight, followed by addition of 1 μL of Turbo DNase (Thermo Fisher Scientific) provided with the kit and incubation at 37 °C for another 15 min. Following a standard protocol, the reaction volume was adjusted to 750 μL with RNase-free water and 0.1 volumes of 3M sodium acetate was added, followed by phenol-chloroform extraction. RNA was then precipitated with two volumes 100 % (v/v) ethanol and washed with 500 μL 70 % (v/v) ethanol. The pellet was air-dried and then re-suspended in 40 μL RNase-free water. The Qubit RNA HS Assay Kit (Thermo Fisher Scientific) was used to quantify guide RNA. Primers used are listed in Table S1.

CRISPR donor DNA preparation

CRISPR donor DNA preparation for yeast strain VL6_48N_cas9_JCVI-syn3.0+1267

Gene *527* was inserted into VL6_48N_cas9_JCVI-syn3.0 between gene *526* and adjacent gene *528* via CRISPR/Cas9. Gene *527* was amplified using PrimeSTAR Max Premix and primers 527_50bp_F and 7.5k_ 50bp_R with 50 bp overlapping each side of insertion sites on the JCVI-syn3.0 genome. Genes *610, 520-522, 602-605* were inserted in VL6_48N_cas9_ JCVI-syn3.0 between genes *609* and adjacent gene *611* via CRISPR/Cas9. Genes *610, 520-522, 602-605* were amplified using PrimeSTAR Max Premix with Pmod2-hisarscen-*610—520-522—602-605* as the template, and primers 610_7.8k_F and 610_7.8k_R with 50 bp overlapping each side of insertion sites on the JCVI-syn3.0 genome. The presence and location of genes were confirmed by obtaining the expected PCR products across junctions (Table S1). Primers are listed in Table S1.

CRISPR donor DNA preparation for yeast strain VL6_48N_cas9_JCVI-syn3.0+2

Gene *527* was inserted into VL6_48N_cas9_JCVI-syn3.0 between gene *526* and adjacent gene *528* via CRISPR/Cas9. Gene *527* was amplified using PrimeSTAR Max Premix, primers 7.5 K 2J R(517) and 7.5 K LJ F(190), and Pmod2-hisarscen-*527_538_546-549_592-593_622-623* as the template. The expected sizes of PCR products listed in Table S1 were obtained. Primers are listed in Table S1.

CRISPR donor DNA preparation for yeast strain VL6_48N_cas9_JCVI-syn3.0+234578

Gene *610* was amplified, with plasmid Pmod2-hisarscen-*610—520-522—602-605* as the template, using PrimeSTAR Max Premix and primers 610_7.8k_F and 610_7.8k_R with 50 bp overlapping each side of insertion sites on the JCVI-syn3.0 genome. Gene *610* was inserted in VL6_48N_cas9_ JCVI-syn3.0 after gene *609* and before gene *611* via CRISPR/Cas9. The genes *527, 538, 546-549, 592-593,* and *622-623* were inserted into VL6_48N_cas9_JCVI-syn3.0 after gene *526* and before *528* via CRISPR/Cas9. Genes *527, 538, 546-549, 592-593,* and *622-623* were amplified with plasmid Pmod2-hisarscen-*527_538_546-549_592-593_622-623* as the template, PrimeSTAR Max Premix, and primers 527_50bp_F and 7.5k_ 50bp_R with 50 bp overlapping each side of insertion sites on the JCVI-syn3.0 genome. Primers are listed in Table S1.

For CRISPR donor DNA preparation, the PCR conditions were: 2 min at 98°C; 30 cycles of 98°C for 10 s, 55°C for 10 s, and 72°C for 1 min; and, followed by 72°C for 3 min.

Yeast transformation and screening

The transformation of yeast, selection, and screening for positive colonies were performed as described elsewhere (Kannan et al., 2016) with some changes. Briefly, 500 ng of donor DNA, (400 to 500) ng guide RNA, and 100 ng PCC1BAC_trp plasmid (GenBank: MN982904) as the selective trp marker (gift from Dr. Billyana Tsvetanova, SGI-DNA, Inc.) were co-transformed with yeast VL6_48N_cas9_JCVI-syn3.0. After electroporation, 1 mL of YPDA/sorbitol media was mixed with cells and transferred to a 30°C shaker for 2 h. 100 μL of culture was plated on selection plates containing CM Glucose Agar, Dry, w/o Histidine, Tryptophan. Colonies appeared after 4 days and diagnostic PCR was run with junction primers to screen positive colonies with genomic modification. The expected sizes of PCR products listed in Table S1 were obtained. For positive clones, multiplex PCR was run to confirm genome integrity. Primers for junction and multiplex PCR are listed in Table S1.

Please cite this article in press as: Pelletier et al., Genetic requirements for cell division in a genomically minimal cell, Cell (2021), https://doi.org/10.1016/j.cell.2021.03.008

Genome transplantation

Mycoplasmal genomes that are maintained and manipulated in yeast as yeast centromeric plasmids can be booted up by genome transplantation into a recipient organism, *Mycoplasma capricolum,* as described in detail elsewhere (Gibson et al., 2010; Hutchison et al., 2016; Lartigue et al., 2009; Tsarmpopoulos et al., 2016). The positive yeast clones containing verified chromosomes were transplanted, as described previously (Lartigue et al., 2009). Single colonies isolated from mycoplasmal transplant outgrowth populations (grown under selection on tetracycline plates) were transferred to SP4 liquid culture without tetracycline. After growth for 3 days, cells were imaged as wet mounts using DIC microscopy to determine morphology.

To confirm the chromosomal constructs in mycoplasmal transplants, genomic DNA was extracted from cells in mid-log phase liquid culture and used as PCR template. The inserted genes were amplified using PCR with PrimeSTAR Max Premix. The PCR conditions were: 2 min at 98°C; 30 cycles of 98°C for 10 s, 55°C for 10 s, and 72°C for 1 min; and, followed by 72°C for 3 min. Zymo DNA Clean & Concentrator Kit purified PCR products were checked using Sanger sequencing and no mutation was found in any of the constructs. The sequencing primers used for these transplants are listed in Table S1.

To confirm genome integrity, QIAGEN Multiplex PCR Kit was used for colony PCR, using primers listed in Table S1. Each pair of forward and reverse primers generated a PCR product specific for a genome segment. The expected product lengths are indicated. The PCR conditions were: 95°C for 15 min; 34 cycles of 94°C for 30 s, 52°C for 90 s, and 68°C for 2 min; followed by 68°C for 3 min. For all PCR, the primers were diluted to 2-10 μmol/L and the final concentration of each primer is 0.1-0.5 μmol/L. Genome manipulation in yeast and transplantation do not induce mutations as shown by sequencing before and after transplantation (Lartigue et al., 2009), and cells were passaged as few generations as possible – typically ≈20 generations – before assaying cell morphology. For experiments using CRISPR/Cas9, guide RNA forward primers and donor DNA oligonucleotides were ordered from IDT.

Gene removal from bacterial genomes in yeast

CRISPR/Cas9 methods were used to delete the following individual gene clusters from VL6_48N_cas9_JCVI-syn3A: *520-522, 610, 602-605, 527, 538, 546-549, 592-593,* or *622-623*. For the methods of production of guide RNA targeting each gene cluster see *CRISPR/Cas9 guide RNA production and quantification* above.

Single stranded donor DNA 100 base oligonucleotides (IDT) were used as a patch to seal the gap after deleting genes *520-522*. The 100 base donor carried two 50 bp overlaps with the two sides of genomic DNA breaks. PCC1BAC_trp plasmid (100 ng), 1 μg of donor DNA, and 500 ng of guide RNA targeting gene *520-522* (see *CRISPR/Cas9 guide RNA production and quantification*) were co-transformed into yeast competent cell VL6_48N_cas9_syn3A. Later positive colonies were screened using a QIAGEN Multiplex PCR Kit. The expected DNA sizes are listed in Table S1. Gene *522* and its 5′ flanking region, gene *521*, and most of *520* were deleted and we obtained VL6_48N_cas9_syn3AΔ*520-522*.

Using the same methods, we obtained the following strains:

- VL6_48N_cas9_syn3AΔ*527* with gene *527* deleted from JCVI-syn3A
- VL6_48N_cas9_syn3AΔ*538* with gene *538* deleted from JCVI-syn3A
- VL6_48N_cas9_syn3AΔ*546-549* with gene *546-549* deleted from JCVI-syn3A
- VL6_48N_cas9_syn3AΔ*592-593* with gene *592-593* deleted from JCVI-syn3A
- VL6_48N_cas9_syn3AΔ*602-605* with gene *602-605* deleted from JCVI-syn3A
- VL6_48N_cas9_syn3AΔ*610* with gene *610* deleted from JCVI-syn3A
- VL6_48N_cas9_syn3AΔ*622-623* with gene *622-623* deleted from JCVI-syn3A

The expected DNA sizes were listed in Table S1. For positive clones with the desired gene deletion, multiplex PCR using a QIAGEN Multiplex PCR Kit was performed to confirm the whole genome integrity, using primers listed in Table S1.

Genome transplantation was carried out to recover the modified JCVI-syn3A strains from yeast and diagnostic PCR and multiplex PCR were used to confirm the insert junctions and genome integrity. Junction primers are listed in Table S1. Primers for gene removal and primers for JCVI-syn3A genome integrity used are listed in Table S1, and the expected DNA amplicons listed in Table S1 were obtained.

Deletion of one gene cluster from JCVI-syn3.0+1267

Strain JCVI-syn3.0+*527+610+520-522+602-605* showed the JCVI-syn3A phenotype. We tried to delete one gene cluster from the strain to obtain the minimal gene number needed to restore the JCVI-syn3A phenotype.

We used CRISPR/Cas9 methods to delete genes from yeast strain VL6_48N_Cas9_JCVI-syn3.0+*527+610+520-522+602-605*. We obtained guide RNA first. To make 520 gRNA2, we designed single guide RNA (sgRNA) targeting the gene *520-522* in JCVI-syn3.0 genome. (119 to 120) bp dsDNA was obtained via PCR with the guide RNA forward primer 520 gRNA2_F (with T7 promoter, (19 to 20) bp guide RNA target, and overlap with 83 bp sgRNA template (Mali et al., 2013)), reverse primer gRNA_R, 83 bp sgRNA template, and PrimeSTAR Max Premix in a 20 μL PCR reaction. The (119 to 120) bp dsDNA was transcribed *in vitro* using T7 RiboMAX Express Large Scale RNA Production System (Promega Corporation) in 20 μL volumes, including 10 μL 2X buffer, 2 μL of T7 RNA polymerase, and 200 ng dsDNA. Guide RNA was purified using Acid-Phenol:Chloroform at pH 4.5 (Thermo Fisher Scientific), precipitated using

Please cite this article in press as: Pelletier et al., Genetic requirements for cell division in a genomically minimal cell, Cell (2021), https://doi.org/10.1016/j.cell.2021.03.008

100 % (v/v) ethanol and 3M sodium acetate, and dissolved in 40 μl RNase free water. A Qubit RNA HS Assay Kit (Thermo Fisher Scientific) was used to quantify guide RNA.

To make VL6_48N_Cas9_JCVI-syn3.0+*527+520-522+602-605+610Δ520-522* (Table S1), gene cluster *520-522* was deleted from yeast strain VL6_48N_Cas9_JCVI-syn3.0+*527+520-522+602-605+610* using CRISPR/Cas9 methods. Briefly. 520 gRNA2 and 520 gRNA3 were used to guide Cas9 protein to the gene *520-522* target sites and cut the genome of JCVI-syn3.0+*527+520-522+602-605+610*, 520 patch was used as the donor DNA to seal the cut, and PRS316 plasmid (bearing the ura3 marker) was used as the selective marker to co-transform the competent yeast strain VL6_48N_cas9_JCVI-syn3.0+*527+520-522+602-605+610*. The transformation reaction mix was incubated at 30°C for 2 h and plated for selection on CM Glucose Broth without Histidine and Uracil c7221 agar medium. The plate was incubated at 30°C for (3 to 4) days, and diagnostic PCR using junction primers was run to screen for positive colonies that had the gene cluster *520-522* deleted using a QIAGEN Multiplex PCR Kit. PCR products with the expected sizes listed in Table S1 were obtained.

Using the same methods, we deleted gene clusters *527*, *602-605* or *610*, to obtain strains JCVI-syn3.0+*527+520-522+602-605+610Δ527*, JCVI-syn3.0+*527+520-522+602-605+610Δ602-605*, and JCVI-syn3.0+*527+520-522+602-605+610Δ610* (Table S1), respectively. The guide RNA forward primers, donor DNA, primers for JCVI-syn3.0 genome integrity, and junction primers are listed in Table S1. PCR products of the expected sizes listed in Table S1 were obtained.

Deletion of genes from JCVI-syn3.0+126 using CRISPR/Cas9

Strain JCVI-syn3.0+*527+520-522+602-605* showed a JCVI-syn3A phenotype. Deletion of gene *527* from JCVI-syn3.0+*527+610+520-522+602-605* caused a reversion to a pleomorphic phenotype, thereby indicating that gene *527* is necessary to confer the JCVI-syn3A phenotype in that strain. Similarly, deletion of the individual gene clusters *520-522* or *602-605* from the strain also rendered the pleomorphic cell phenotype. We therefore sought to determine the effect of removing the individual genes within these three clusters on the JCVI-syn3A phenotype of strain JCVI-syn3.0+*527+520-522+602-605*. CRISPR/Cas9 methods were used in a yeast strain carrying JCVI-syn3.0+*527+520-522+602-605* to delete single genes, or gene pairs, from the genome of JCVI-syn3.0+*527+520-522+602-605* in yeast. The yeast strain VL6_48N_cas9_JCVI-syn3.0+*527+520-522+602-605* (carrying the *trp* plasmid and *ura3* plasmid from previous experiments) was passaged twice (with 1:1000 dilution), grown in CM Glucose Broth without Histidine liquid media for 24 h, and then diluted and plated on separate agar plates containing CM Glucose Broth: (i) without Histidine; (ii) without Histidine and Tryptophan; or, iii) without Histidine and Uracil. Yeast colonies growing only on CM Glucose Broth without Histidine were picked. Trp and ura3 markers were absent from these clones, and one was used for the following experiments.

For gene cluster *520-522,* there were 6 deletion combinations, including deletion of gene *520*, *521* or *522*, *520+521*, *521+522*, or *520+522*. For gene cluster *602-605,* there are also 6 deletion combinations, including deletion of gene *602*, *604*, *605*, *602-604*, *604+605*, or *602+605*. Note that locus tag _0603 is no longer annotated as a gene; rather, it represented a small region of DNA 5′ of gene *604.*

To generate some mutants, we used the same CRISPR/Cas9 methods to remove genes, except that donor DNA was produced via PCR. To make JCVI-syn3.0+*527+520-522+602-605Δ521*, we used primers 521-40bpR and 520 jump F1, JCVI-syn1.0 genomic DNA as the template, and PrimeSTAR Max Premix in a PCR to produce a 730 bp DNA donor. To make JCVI-syn3.0+*527+520-522+602-605Δ602Δ605* or JCVI-syn3.0+*527+520-522+602-605Δ605,* we used PCR primers 604-40-F1 and 604-40-R1, JCVI-syn1.0 genomic DNA as template, and PrimeSTAR Max Premix. To make JCVI-syn3.0+*527+520-522+602-605Δ520Δ522,* we used PCR primers 521-40bp-R, 521-40bp-F, JCVI-syn1.0 genomic DNA as the template, and PrimeSTAR Max Premix to produce a 760 bp DNA donor. To make JCVI-syn3.0+*527+520-522+602-605Δ604*, a 500 bp donor DNA was made via a fusion PCR. First, we used primers 602jumpF2(315) and 604-40bpR, to obtain a 516 bp PCR product. Next, the PCR product was purified using a Zymo DNA Clean & Concentrator Kit. At the same time, primers 604-80bp and 602jumpR3(492), Syn1.0 genomic DNA as the template, and PrimeSTAR Max Premix were used for PCR to yield a 480 bp PCR product, which was the purified using a Zymo DNA Clean & Concentrator Kit. 20 ng of each of the above two PCR products, primers 602jumpF2(315) and 602jumpR3(492), and PrimeSTAR Max Premix were used to produce 996 bp donor DNA. The PCR conditions were: 98°C for 3 min; 30 cycles of 98°C for 10 s, 55°C for 10 s, 72°C for 1 min, and, followed by 72°C for 2 min. The PCR amplicon was purified using a Zymo DNA Clean & Concentrator Kit. 500 ng each of guide RNA 602 gRNA3, 605 gRNA1, 604 gRNA2, as well as 1 μg of donor DNA and 100 ng PCC1BAC_trp plasmid, were used to transform yeast competent cells.

To delete gene *520* from the genome of JCVI-syn3.0+*527+520-522+602-605* in yeast (Table S1), 520 gRNA3 was used to guide Cas9 protein to the 520 gRNA3 target site and cut the genome of JCVI-syn3.0+*527+520-522+602-605*. Single-stranded oligonucleotide 520-80 base patch was used as donor DNA to seal the cut, and PCC1BAC_trp plasmid was used as the selective marker to co-transform the competent yeast strain VL6_48N_cas9_JCVI-syn3.0+*527+520-522+602-605*. The transformation reaction mix was incubated at 30°C for 2 h and plated on a selective plate with CM Glucose Broth without Histidine and Tryptophan. The plate was incubated at 30°C for (3 to 4) days, and diagnostic PCR using junction primers was run to screen positive colonies that had the gene *520* deleted. The expected DNA sizes of PCR products listed in Table S1 were obtained. The yeast strain with gene *520* deleted was used for genome transplantation to generate a mycoplasmal transplant with the genome of JCVI-syn3.0+*527+520-522+602-605Δ520*. Junction PCR results confirmed that gene *520* was deleted.

Using the same method, we obtained the following strains:

Please cite this article in press as: Pelletier et al., Genetic requirements for cell division in a genomically minimal cell, Cell (2021), https://doi.org/10.1016/j.cell.2021.03.008

- JCVI-syn3.0+527+520-522+602-605Δ602
- JCVI-syn3.0+527+520-522+602-605Δ602-604
- JCVI-syn3.0+527+520-522+602-605Δ604-605
- JCVI-syn3.0+527+520-522+602-605Δ522
- JCVI-syn3.0+527+520-522+602-605Δ520-521
- JCVI-syn3.0+527+520-522+602-605Δ521-522

QUANTIFICATION AND STATISTICAL ANALYSIS

Empirical gradient thresholding to estimate cell size distributions

Size distributions were quantified using the empirical gradient threshold (EGT) algorithm to binarize grayscale images (Chalfoun et al., 2015).

CellPress

Supplemental figures

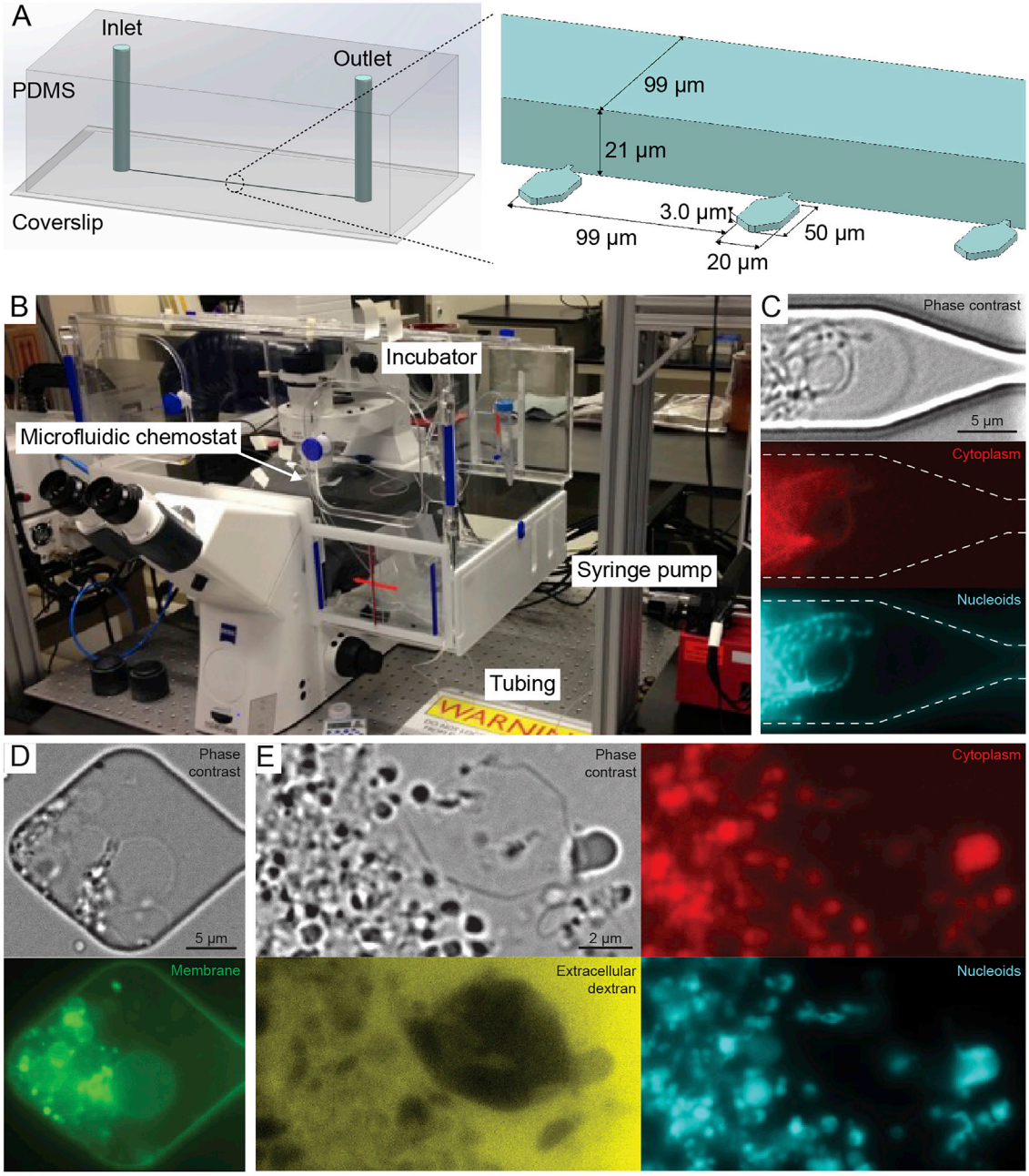

Figure S1. Microfluidic chemostat isolates cells from shear flow to image their intrinsic morphological dynamics and cellular composition during growth and propagation, related to Figures 1, 3, and 4

(A) The microfluidic chemostat is shown schematically with internal dimensions. Cells grow in chambers, in diffusive contact with a flow channel that provides a continuous supply of fresh growth medium. (B) Microfluidic chemostat, shown within the complete laboratory setup, includes the syringe pump and incubator. Brightfield and fluorescence optical micrographs of RGD6+mCherry grown in microfluidic chambers show filamentous cells (C), and large cells and vesicles (D,E). (C) Nucleoids appeared separated along the length of filamentous cells, suggesting genome segregation may continue in the absence of complete cell scission, as recently observed in *B. subtilis* L-forms (Wu et al., 2020). (D) The surface of vesicles, which appeared as lower contrast in phase contrast images, were stained with the membrane dye SP-DiOC18(3). (E) A large vesicle lacked constitutively expressed mCherry but excluded FITC-conjugated dextran in the growth medium, suggesting the vesicle membrane was not permeable to macromolecules.

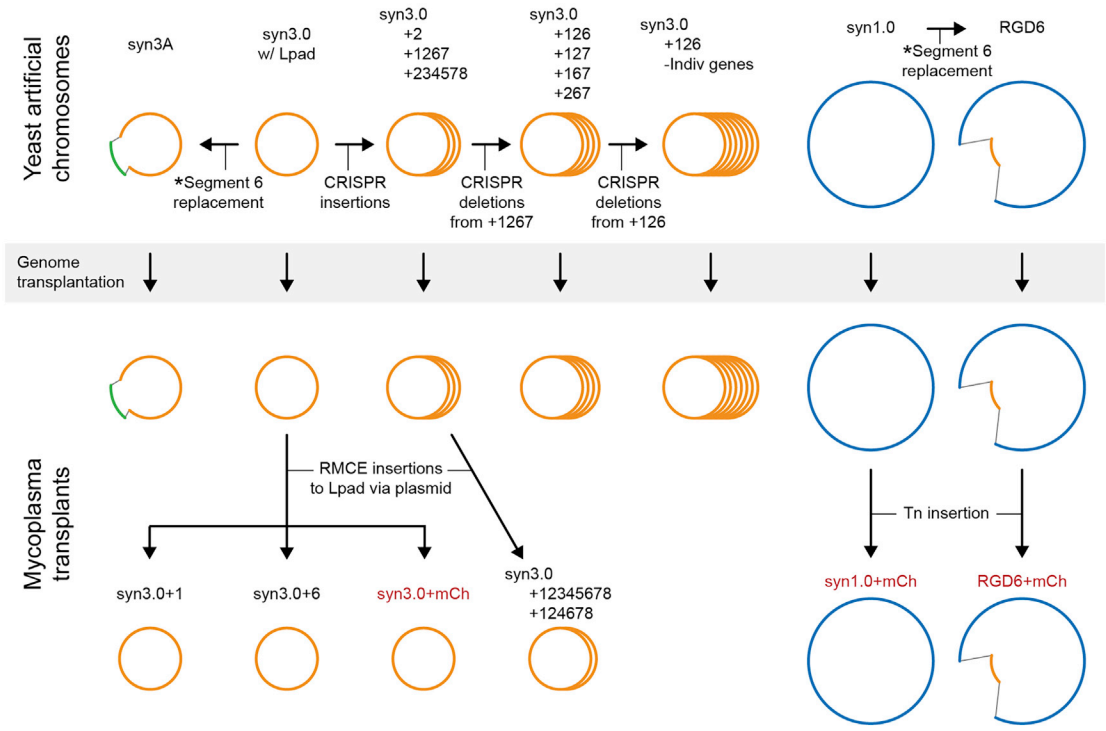

Figure S2. Overview of genomic manipulations to generate strains reported in this study, related to STAR Methods

Genomes were manipulated using two strategies: (1) For artificial chromosomes in yeast (upper constructs) CRISPR/Cas9 (CRISPR) methodology was used to generate insertions/deletions, followed by genome transplantation into a mycoplasma recipient to render mycoplasmal organisms programmed with the new genome; or, (2) for chromosomes in the mycoplasmal transplants (lower constructs), recombination mediated cassette exchange (RMCE) was used to introduce genes transferred from plasmids to a chromosomal landing pad (Lpad) comprising heterospecific *loxP* sites. In cases where the landing pad was absent (JCVI-syn1.0 and RGD6), a gene encoding the fluorescent protein mCherry was introduced by transposome mediated insertion. The key gene clusters transferred, numbered 1 through 8, correspond to those indicated in Figure 5 of the article. The content of gene clusters within each strain or group of strains is indicated according to the designations in Figure 5. A group of strains (tiled circles) with different combinations is indicated by listing the combinations represented. Arrows represent a manipulation from one strain to another. Arrows in the shaded area indicate genome transplantations. Details of these processes are described in STAR Methods. *Methods for replacement of genomic segments, as well as the construct RGD6, are detailed elsewhere (Hutchison et al., 2016). The full sequence and annotation of segment 6 in JCVI-syn3A is provided in the whole genome sequence (GenBank: CP016816.2).

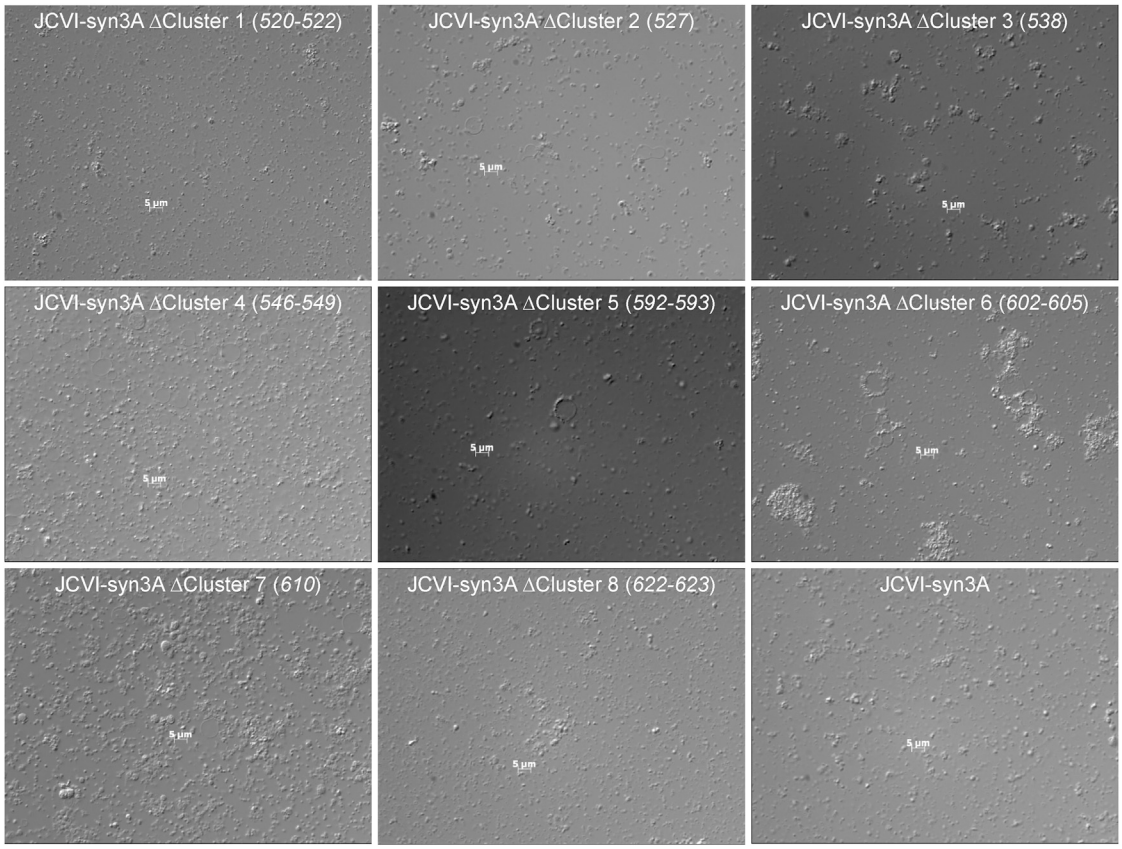

Figure S3. Deletion of genes or gene clusters from JCVI-syn3A, related to Figure 5

Surprisingly, JCVI-syn3A retained a nearly normal morphology after the deletion of cluster 1 (*520-522*), despite the requirement for cluster 1 for the nearly normal morphology in JCVI-syn3.0+126. Strains were classified as normal morphology or pleomorphic by scanning samples for large pleomorphic forms and imaging them, if present. Therefore, these images are representative of a much greater number of cells, and the classification as normal morphology is stringent.

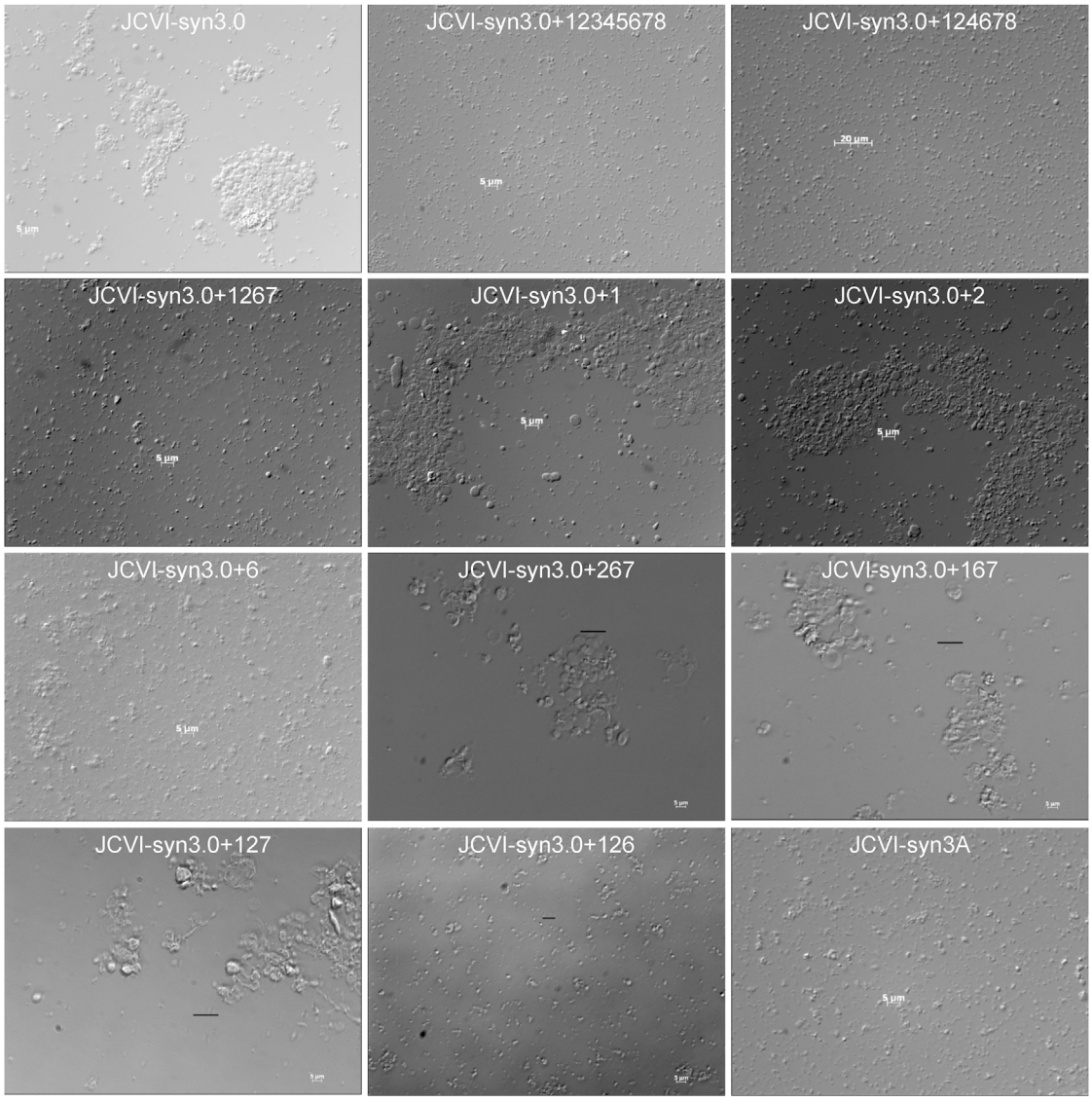

Figure S4. Addition of genes or gene clusters to JCVI-syn3.0, related to Figure 5

Addition of cluster 1 (*520-522*), cluster 2 (*527*), and cluster 6 (*602,604,605*) was necessary to restore a nearly normal morphology in JCVI-syn3.0+126. These same strains are listed in Figure 5C of the main text. Strains were classified as normal morphology or pleomorphic by scanning samples for large pleomorphic forms and imaging them, if present. Therefore, these images are representative of a much greater number of cells, and the classification as normal morphology is stringent. Black bars in some panels are residual annotations superimposed by image analysis software.

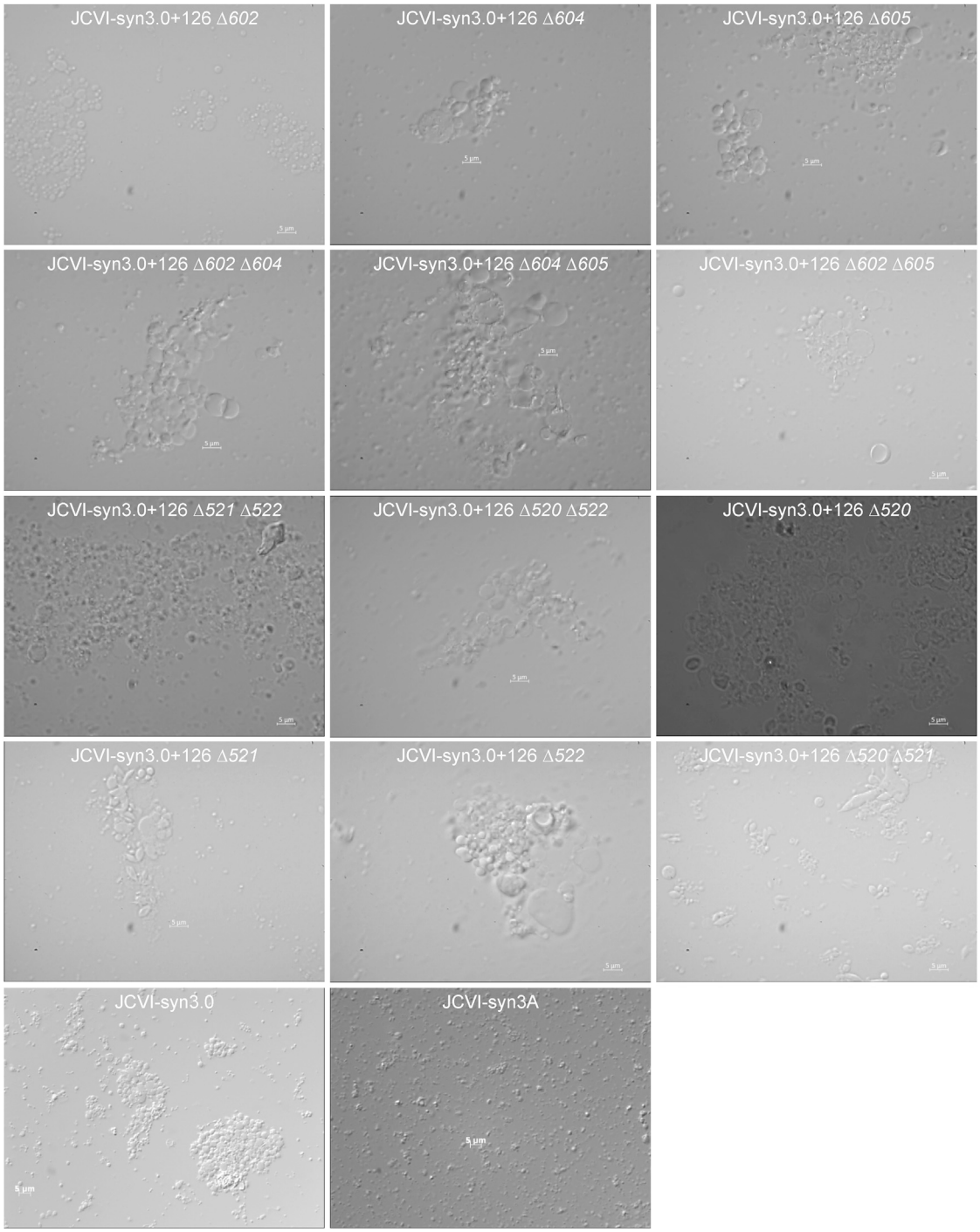

Figure S5. Deletion of genes or gene pairs from JCVI-syn3.0+126, related to Figure 5

Deletion of any of the seven genes (*520*, *521*, *522*, *527*, *602*, *604*, or *605*) from JCVI-syn3.0+126 caused loss of the nearly normal morphology. Strains were classified as normal morphology or pleomorphic by scanning samples for large pleomorphic forms and imaging them, if present. Therefore, these images are representative of a much greater number of cells, and the classification as normal morphology is stringent.